

Liquid Metal + x: A Review of Multiphase Composites Containing Liquid Metal and Other (x) Fillers

Sophia Eristoff, Amir Mohammadi Nasab, Xiaonan Huang, and Rebecca Kramer-Bottiglio*

Multiphase mixtures containing both liquid metal and solid inclusions in a soft polymeric matrix can exhibit unique combinations of mechanical, electrical, magnetic, and thermal properties. Gallium-based liquid metals have excellent electrical and thermal properties, and incorporating additional conductive, magnetic, or other solid fillers into liquid metal-embedded elastomers can yield heightened electrical and thermal conductivities, enhanced elasticity due to lowered percolation thresholds, and positive piezoconductivity. This emerging class of liquid metal + x composites, where x denotes any solid filler type, has applications in stretchable electronics, wearables, soft robotics, and energy harvesting and storage. In this review, the recent literature is consolidated on liquid metal + x composites and their potential to offer uniquely amplified or multiplied bulk properties is highlighted. The literature related to the materials and processing of liquid metal + x composites is reviewed, through which it is found that the properties of the resulting multiphase composites are sensitive to the sequence in which the distinct liquid metal and solid inclusions are incorporated into the continuous phase. This review further includes a summary of relevant predictive modeling approaches, as well as identifies grand challenges and opportunities to advance liquid metal + x composites.

although there exists a T_m range depending on processing and formulation^[2,3]—liquid metals boast low toxicity,^[4] low viscosity, exceptional electrical, and thermal conductivity, high deformability, self-healing capability, near-zero vapor pressure, and voltage-responsive interfacial energy.^[5–7] The interfacial energy of liquid metals is dominated by surface gallium oxidation,^[8] which forms a stable amorphous oxide film that has presented both processing challenges and incredible shape stability.^[9] Given such properties, it is unsurprising that liquid metals have emerged as a leading candidate material for applications including stretchable conductors,^[10] electrodes and batteries,^[11] sensors,^[12–16] antennas,^[17] transistors,^[18,19] memristors,^[20] energy harvesting devices,^[21–23] soft actuators,^[24] and integrated circuits.^[25,26]

Incorporating liquid metal inclusions into solid-phase materials generates liquid metal composites, which have been shown to impart many of the unique and advantageous properties of liquid metal to bulk solids. For example, Ford et al.^[27]

1. Introduction

Gallium-based alloys that are liquid at room temperature, or liquid metals (LM), are a fascinating class of materials with highly unique properties.^[1] Most commonly, liquid metals refer to eutectic gallium indium (eGaIn; 75% Ga and 25% In by weight) or Galinstan (68.5% Ga, 21.5% In, and 10% Sn by weight). Along with their sub-room temperature melting point—nominally $T_m = 15$ °C and -19°C for eGaIn and Galinstan, respectively,

reported liquid metal inclusions in liquid crystal elastomer (LCE) actuators, which imparted conductivity without degrading the mechanical and shape-morphing properties of the LCE. Markvicka et al.^[28] proposed liquid metal droplets suspended in soft elastomer, which, when coalesced via strain or pressure, formed stretchable elastomer conductors. Similarly, Thrasher et al.^[29] presented core-shell particles of liquid metal with surface-bound acrylate ligands that polymerized together to create cross-linked particle networks, which when stretched, form stretchable conductors with a suppressed electromechanical response. Bartlett et al.^[30] showed the enhancement of thermal conductivity in elastomers via liquid metal inclusions.

Recently, researchers have proposed increasingly complex liquid metal composites, often adding additional fillers to either amplify or multiply the functional properties. In this class of composites, liquid metal can bridge between solid fillers to reduce percolation thresholds,^[31] forge inclusion alignments for anisotropy,^[32] or mitigate the compliance mismatch between rigid fillers and soft polymers to reduce stress concentration points that impact the extensibility of the matrix and longevity of the composite.^[33] The emergent benefits of composites containing liquid and solid inclusions have summarily shown integrated

S. Eristoff, A. M. Nasab, R. Kramer-Bottiglio
School of Engineering & Applied Science
Yale University
New Haven 06250, USA
E-mail: rebecca.kramer@yale.edu

X. Huang
Robotics Department
University of Michigan
Ann Arbor 48109, USA

 The ORCID identification number(s) for the author(s) of this article can be found under <https://doi.org/10.1002/adfm.202309529>

DOI: 10.1002/adfm.202309529

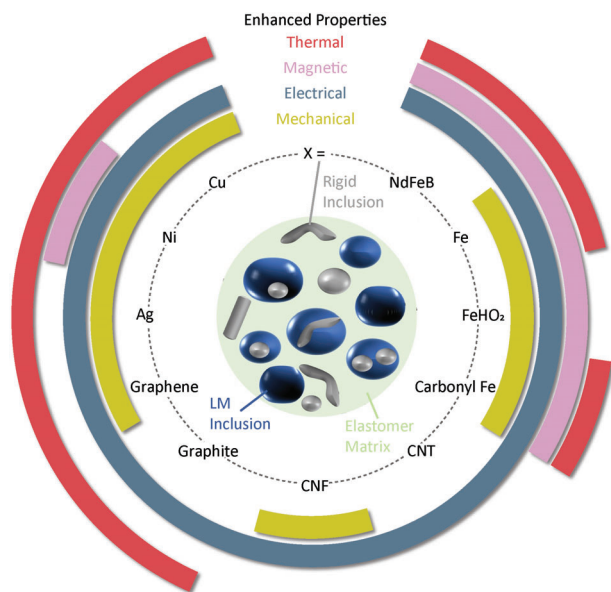


Figure 1. Liquid metal + *x* composites, which are multiphase composites containing both liquid metal inclusions and other solid (*x*) fillers. The outer rings indicate which integrated properties are enhanced or enabled in the liquid metal + *x* composites based on their solid filler. CNF and CNT denote carbon nanofibers and carbon nanotubes, respectively.

mechanical,^[34–36] electrical,^[37–39] magnetic,^[40,41] thermal,^[42,43] self-healing,^[44–47] rheological,^[48] or tribological^[49] properties in synergy with their liquid-solid-reinforced structures.^[50]

The purpose of this review is to highlight the immense potential for liquid metal (LM) + *x* multiphase composites, where “*x*” denotes any solid filler (**Figure 1**). We note that the term ‘multiphase composite’ has been used in the literature to refer to polymer composites containing two or more types of liquid inclusions^[51] or solid fillers,^[52] as well as inclusions of different sizes or shapes of the same material.^[53] Here, we identify multiphase composites containing both liquid and solid inclusions and further narrow our focus to those containing liquid metals. This review complements other recent reviews that focus on composites containing liquid inclusions other than liquid metal,^[54,55] composites containing only liquid metal inclusions,^[56–59] liquid metal particles,^[60–63] and liquid metal fibers.^[64] We exclude complex-phase capsules as composites on their own unless they are embedded into host matrices. Thus, our aim is to report the collective literature on “liquid metal + *x*” composites to elucidate the potential to amplify or multiply bulk properties by adding liquid metal to existing filler-matrix composite materials, as shown in **Table 1**. We further review the materials, processing, and modeling challenges associated with such multi-inclusion composites.

2. Integrated Properties

There are two ways to consider a LM + *x* multiphase composite: 1) a solid filler-matrix composite with added liquid metal, or 2) a liquid metal-matrix composite with added solid filler. In **Table 1**, we consider the literature based on the latter approach, thus grouping composites by *x* and listing their increased or added proper-

ties relative to liquid metal-only composites of the same liquid metal loading percentage. In the following sections, we group LM + *x* composites in the literature by their enhanced or added mechanical, electrical, thermal, and magnetic properties. As a versatile material with excellent electrical and thermal properties, adding liquid metal inclusions to existing composites has been shown to enhance or enable electrical and/or thermal conductivity, often while also introducing favorable or maintained mechanical and/or magnetic properties.

2.1. Mechanical Properties

The mechanical properties of polymers are generally impacted by adding solid or liquid fillers. For example, the addition of solid fillers in a polymer network typically reduces the elasticity and embrittles the network, but may increase the strength of the system.^[33,98–100] The addition of liquid fillers can increase the toughness of the network, as well as enhance energy absorption due to increased energy dissipation via the liquid inclusions.^[5,25,60,101] However, liquid inclusions at high concentrations in a polymer network may induce leakiness when subjected to pressure gradients.^[68,87]

Together, both liquid and solid inclusions in a polymer network create complex interactions, and the specific composition determines whether the liquid or solid inclusions are more dominant toward the bulk mechanical properties. Tutika et al.^[68] studied the mechanical and functional tradeoffs in multiphase composites including both liquid and solid inclusions, yielding an optimized composition of solid conductive particles and eGaIn liquid metal in a silicone matrix with high compliance and thermal conductivity. In some cases, the unique interactions between liquid and solid inclusions extend beyond mitigating the effects of one another and instead create unexpected outcomes. For example, in a work by Bury and Koh,^[69] Galinstan and BTO particles were embedded in a polydimethylsiloxane (PDMS) matrix to yield a stretchable dielectric material, and increasing the Galinstan content was found to increase the composite’s modulus and viscosity—the opposite correlation from what is expected when typically adding liquid filler to a polymer.

Other examples of LM + *x* composites have demonstrated enhanced or added mechanical properties such as increased Young’s modulus,^[68–70,76,78] shear hardening,^[73] increased ultimate strain,^[68] enhanced storage moduli,^[69,71] and decreased gauge factor.^[87] For example, by mixing both Fe particles and liquid metal into a polymer matrix, the toughness and Young’s modulus of the bulk composite can be enhanced.^[69,70,102] Incorporating carbon nanotubes (CNT),^[73–75] carbon nanofibers (CNF),^[76] and graphene flakes^[78–80] with liquid metal into elastomers can also enhance the toughness of the composite. In a work that we find particularly interesting, Saborio et al.^[80] showed that the elastic modulus of a graphene-liquid metal composite initially increases as the loading content of graphene is raised to 1.4 wt.%, then subsequently decreases with further graphene loading to 3 wt.%. Such non-monotonic dependency between solid filler content and elastic modulus is attributed to the flow of liquid metal into cavities, which reduces the friction between the matrix and solid filler, as depicted in **Figure 2A** (and further investigated in other works^[56,103]). However, when the graphene

Table 1. Liquid metal + x composites and their modified or multiplied properties relative to liquid metal-only composites of the same liquid metal loading percentage.

x	Filler type	Matrix	Investigated properties	Reference
NdFeB	particles	Sylgard 184	Added magnetic properties	Zhang <i>et al.</i> ^[65]
NdFeB	particles	Metal-coated particles in liquid metal	Increased thermal and electrical conductivity; added magnetic properties	Lu <i>et al.</i> ^[66]
NdFeB	particles	Sylgard 184	Added magnetic properties	Guan <i>et al.</i> ^[67]
Fe	particles	Gelest PDMS	Increased thermal conductivity, Young's modulus, and ultimate strain	Tutika <i>et al.</i> ^[68]
Fe or BTO	particles	Gelest PDMS	Increased torsion storage modulus, Young's modulus, and dielectric permittivity	Bury and Koh ^[69]
FeHO ₂	particles	Sylgard 184	Added positive piezoconductivity; increased electrical conductivity and Young's modulus	Zhang <i>et al.</i> ^[70]
Carbonyl Fe	particles	Sylgard 184	Added positive piezoconductivity and magnetic properties; increased thermal conductivity	Yun <i>et al.</i> ^[40]
Carbonyl Fe	particles	Sylgard 184	Increased thermal conductivity and storage modulus; added magnetic properties	Li <i>et al.</i> ^[71]
Carbonyl Fe	particles	Sylgard 184	Added magnetic properties and metallic conductivity	Kim <i>et al.</i> ^[72]
Carbon (CNT) and Carbonyl Fe	nanotubes and particles	PDMS-polyurethane blend	Increased electrical conductivity; added electrical self-healing, magnetic properties, and shear hardening	Ding <i>et al.</i> ^[73]
Carbon (CNT)	nanotubes	Sylgard 184	Increased electrical conductivity	Guan <i>et al.</i> ^[74]
Carbon (CNT)	nanotubes	Sylgard 184	Increased electrical conductivity	Li <i>et al.</i> ^[75]
Carbon (CNF)	nanofibers	Sylgard 184	Increased Young's modulus and tensile strength; added strain hardening and positive piezoconductivity; decreased electrical conductivity	Zhang <i>et al.</i> ^[76]
Graphite	flakes	EcoFlex 00-50	Increased electrical and thermal conductivity	Bilodeau <i>et al.</i> ^[31]
Graphite	flakes	EcoFlex 00-30	Increased electrical and thermal conductivity	Li <i>et al.</i> ^[77]
Graphene	nanoplatelets	Sylgard 184	Increased thermal conductivity and Young's modulus	Sargolzaeiaval <i>et al.</i> ^[78]
Graphene	nanoplatelets	Sylgard 184	Increased thermal conductivity	Sargolzaeiaval <i>et al.</i> ^[79]
Graphene	flakes	Sylgard 184	Increased electrical and thermal conductivity; non-monotonic Young's modulus	Saborio <i>et al.</i> ^[80]
Polydopamine-Coated Graphene Oxide	flakes	Sylgard 184	Increased dielectric permittivity; decreased breakdown strength	Hu and Majidi ^[81]
Ag	particles	Silicone oil	Increased thermal conductivity	Uppal <i>et al.</i> ^[82]
Ag	particles	Gelest PDMS	Increased thermal conductivity	Uppal <i>et al.</i> ^[83]
Ag	particles	Poly(styrene-butadiene-styrene) (SBS)	Increased electrical conductivity	Liu <i>et al.</i> ^[84]
Ag	particles	Gelest PDMS	Increased thermal conductivity and Young's modulus	Tutika <i>et al.</i> ^[68]
Ag	flakes and particles	Ethylene vinyl acetate (EVA)	Increased electrical conductivity	Wang <i>et al.</i> ^[85]
Ag	flakes	Styrene-isoprene block copolymer (SIS)	Increased electrical conductivity; non-smearing	Reis <i>et al.</i> ^[86]
Ag	flakes	SIS	Increased electrical conductivity; decreased electromechanical gauge factor; non-smearing	Lopes <i>et al.</i> ^[87]
Ag	flakes	SIS	Increased electrical conductivity; non-smearing	Sgotti <i>et al.</i> ^[88]
Ag	flakes	SIS	Increased electrical conductivity	Hajalilou <i>et al.</i> ^[89]
Ag-coated Silica Carbide	particles	Silicone oil	Increased thermal conductivity	Kong <i>et al.</i> ^[90]
Ag-coated Fe ₂ O ₃	particles	SIS	Increased electrical conductivity	Hajalilou <i>et al.</i> ^[89]

(Continued)

Table 1. (Continued).

x	Filler type	Matrix	Investigated properties	Reference
Ag-coated Ni	particles	SIS	Increased electrical conductivity	Hajalilou <i>et al.</i> ^[89]
Ag-coated Ni	particles	EcoFlex 00-30	Increased electrical conductivity; added magnetic properties	Hoang <i>et al.</i> ^[91]
Ni	particles	SIS	Increased electrical conductivity; decreased electromechanical gauge factor; non-smearing	Hajalilou <i>et al.</i> ^[92]
Ni	flakes	Gelest PDMS	Increased thermal conductivity and Young's modulus	Tutika <i>et al.</i> ^[168]
Ni	flakes	Carboxylated polyurethane	Increased electrical conductivity; added electrical self-healing	Park <i>et al.</i> ^[93]
Ni	flakes	EcoFlex 00-30	Added positive piezoconductivity; increased electrical conductivity and Young's modulus	Zhang <i>et al.</i> ^[70]
Ni	particles	Sylgard 184	Added positive piezoconductivity, magnetic properties; increased thermal conductivity	Yun <i>et al.</i> ^[140]
Ni	spike-shaped particles	Sylgard 184, EcoFlex 00-30	Increased electrical conductivity; added positive piezoconductivity; increased thermal conductivity	Yun <i>et al.</i> ^[94]
Cu	particles	Thermoplastic elastomer	Increased thermal and electrical conductivity; non-smearing	Chen <i>et al.</i> ^[95]
Cu	particles	Polymer-coated particles in liquid metal	Increased thermal conductivity	Zhang <i>et al.</i> ^[96]
Cu	particles	EcoFlex 00-30	Increased thermal conductivity and Young's modulus	Zhang <i>et al.</i> ^[97]
Cu	particles	Gelest PDMS	Increased thermal conductivity and Young's modulus	Tutika <i>et al.</i> ^[168]

loading is increased beyond 3 wt.%, direct contact between flakes promotes van der Waals interactions, thus reverting the dependency between solid filler content and elastic modulus back to a positive correlation.

Another favorable mechanical property in LM + x composites is non-smearing, which may be useful in scenarios where encapsulation of a material is not possible or favorable.^[87] Frequently, liquid metal composites leak as the liquid metal percolates out of the network. However, the addition of solid metal filler particles can act as a strong anchor for liquid metal to prevent smearing on the composite's surfaces.^[86–88] Liquid metals have been shown to reactively wet or otherwise adhere to solid metals such as Ag, Au, Cr, Cu, Fe, and Ni, and the inclusion of these filler types in composites can thus “hold” the liquid metal in place.^[84,87,104–106] For example, in Lopes *et al.*,^[87] Ag nanoparticles were mixed with eGaIn and styrene-isoprene block copolymer (SIS) to form a conductive non-smearing composite. The addition of the silver nanoparticles slightly enhances the electrical conductivity of the composite, but more favorably imparts a solid-like integrity seen in just solid-phase composites, which prevents smearing. Such non-smearing surfaces could lend toward applications in the actuator space, such as thermo-responsive actuators^[88] or dielectric elastomer actuators (DEAs)^[86] (see Figure 2B), where smearing of conductive traces (as shown for the carbon black and carbon grease traces in Figure 2B) can often lead to electrical shorting or other catastrophic failures.

2.2. Electrical Properties

Imbuing soft polymers with conductive fillers is a common approach to stretchable conductors, which are essential components for emerging wearable and soft robotic technologies.

Either conductive solid or liquid inclusions could be used to achieve electrical conductivity in a polymer. Solid fillers such as silver or copper are commonly used due to their high electrical conductivity, but often require high loading to achieve percolation.^[85] The percolation threshold, or the volume fraction of conductive filler required to achieve bulk conductivity, is sensitive to the size and geometry of the particles.^[36] Spherical particles contribute to a very high percolation threshold since all of the particulate mass is concentrated into isolated spheres of low aspect ratio. Particles with an amorphous geometry typically enable a lower percolation threshold. Generally, high loading of solid filler leads to bulk embrittlement, which is often unfavorable for conductive polymers. Conductive liquid fillers, such as ionic fluids and liquid metals, can impart electrical conductivity to their polymer hosts without embrittlement. Liquid inclusions typically require lower loadings to achieve percolation when compared to their solid counterparts, as they are able to flow and form conductive pathways.^[23,29] However, liquid inclusions are often leaky, which can result in unreliable conductivity and mechanical properties with compliance degrading at high loadings.^[68,86–88]

The combination of both conductive liquid and conductive solid inclusions can reduce percolation thresholds and mitigate negative properties often seen with single-phase composites.^[40,68,85] While ionic liquids have been used in electrically conductive multiphase composites,^[107] the majority of multiphase electrically conductive polymer composites are manufactured by incorporating liquid metal and small amounts of conductive rigid inclusions with high aspect ratios such as silver,^[84–89] nickel,^[70,91–94] graphite,^[31,77] graphene,^[80] and carbon nanotubes.^[73–75] The synergy between both liquid metal and the conductive solid (x) fillers yields a balanced blend that

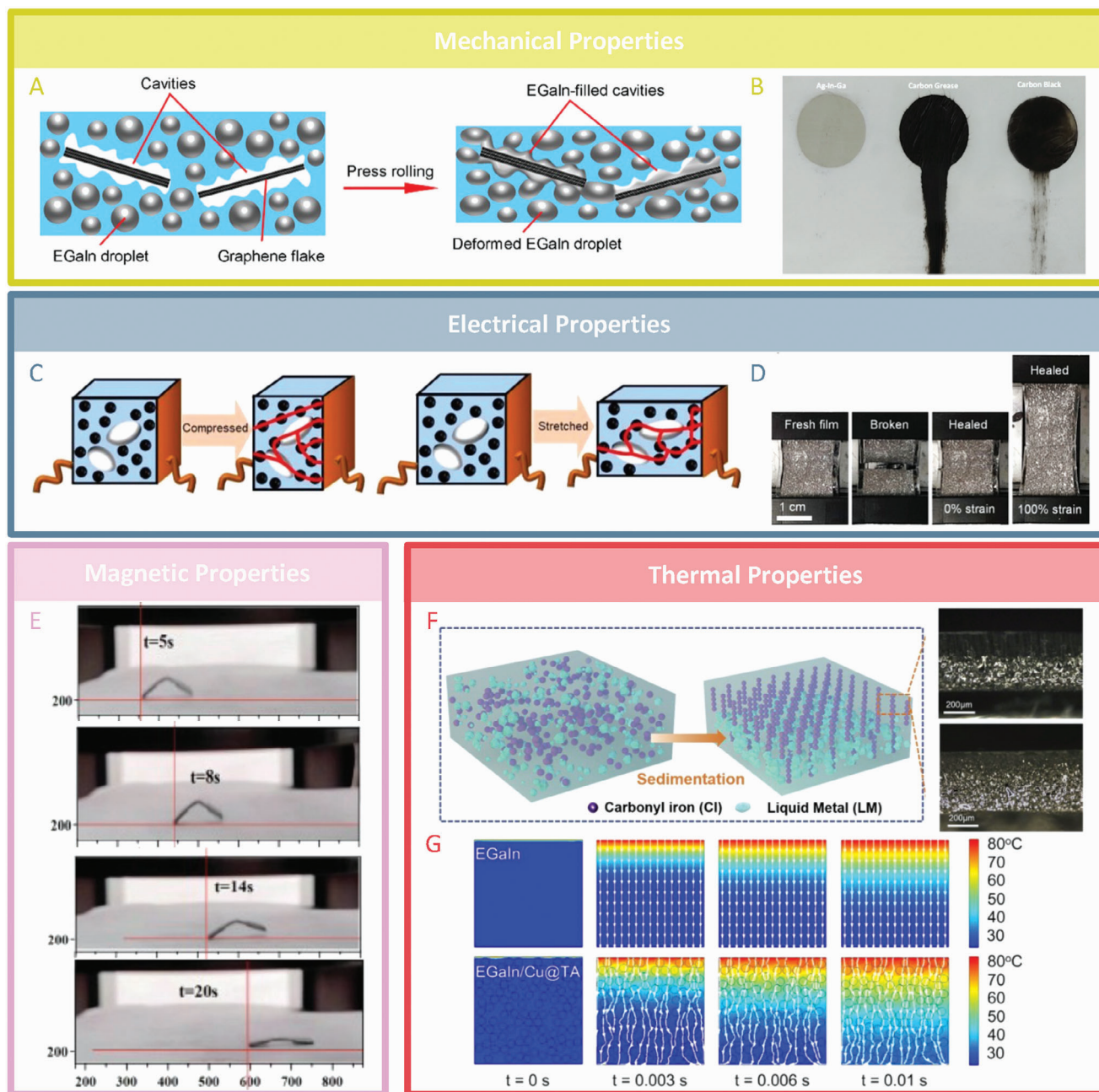


Figure 2. Examples of liquid metal (LM) + x composites and their enhanced or enabled mechanical, electrical, magnetic, and thermal properties. A) Schematic of effects of compression on a LM + x composite. Under compression, the LM flows into the cavities formed around the graphene (x), enhancing the mechanical and electrical properties of the composite. Reproduced with permission.^[80] Copyright 2019, Wiley-VCH. B) Images of electrodes used for dielectric elastomer actuators made using a non-smearing LM + x composite, and smearing carbon grease and carbon black. Reproduced with permission.^[86] Copyright 2021, Wiley-VCH. C) Schematic of the positive piezoconductivity achieved under deformation when using a LM + x composite. Reproduced with permission.^[70] Copyright 2021, IOP. D) Images of a LM + x composite and its self-healing properties. Post-healing, the material exhibits electrical self-healing under strain due to the flow of LM into the healed zone. Reproduced with permission.^[93] Copyright 2018, Wiley-VCH. E) Images of an inchworm-inspired magneto-responsive LM + x composite locomoting in response to a magnetic field. The x-axis units are mm. Reproduced with permission.^[67] Copyright 2023, Elsevier. F) Schematic of the effects of adding magneto-responsive fillers to a LM-PDMS composite. Cross-sectional optical microscopy images show the composite without and with a magnetic field applied during curing on the top and bottom, respectively. Reproduced with permission.^[71] Copyright 2023, Elsevier. G) Finite elemental analysis (FEA) images of a LM + x composite (bottom) and its heat flux transport compared to just pure LM (top). Reproduced with permission.^[96] Copyright 2023, Wiley-VCH.

co-optimizes the composite's bulk mechanical and electrical properties.

In LM + x composites, the liquid metal often acts as the secondary contributor to electrical conductivity. Solid fillers are typically unable to achieve percolation alone, except at very high loadings. However, at high strains, liquid metal can percolate into the gaps between the solid fillers and bridge an electrical network. For example, Wang et al.^[85] described a superelastic conductor with an initial conductivity of 8331 S cm⁻¹ and a maximum strain of 1000%, achieved using both Ag flakes and eGaIn particles in a polymer matrix. When subject to strain, the eGaIn particles rupture, maintaining the electrical connections between the Ag flakes. The eGaIn particles act as electrical anchors for the Ag flakes, but due to their liquid state, preserve the stretchability of the composite. In Hajalilou et al.,^[89] a variety of LM + x composites were probed and optimized to combine the best properties of liquid metal composites with the best properties of solid filler composites. A mixture of eGaIn and Ag flakes yielded the highest conductivity with optimized mechanical properties, as compared to composites containing eGaIn and x = {Fe, Ni, Ag-coated Ni, or Ag-coated Fe}.

Electrical resistivity usually increases by stretching a conductive material, as interconnects between electrically conductive fillers reduce in magnitude.^[108–110] However, in certain LM + x composite cases, added positive piezoconductivity results in electrical resistivity decreasing as tensile strain increases, which is a fascinating and under-explored phenomenon.^[40,70,94] In Yun et al.,^[40] the electrical resistivity of a Fe-eGaIn-PDMS composite drops by three orders of magnitude during strain, exhibiting positive piezoconductivity. The unique piezoconductivity properties of the Fe-eGaIn-PDMS composite are attributed to the deformation of eGaIn particles, and lack thereof of Fe particles, during strain. Under strain, the Fe particles may compress against the PDMS matrix and eGaIn, leading to an overall reduction in the thickness of the PDMS layer and a potential increase in Fe-eGaIn contacts, which in turn decreases resistivity, as shown in Figure 2C. This positive piezoconductivity is also apparent in Zhang et al.^[70] and Yun et al.,^[94] where the unusual positive piezoconductivity property is used for a variety of sensing applications.

When tuning the electrical conductivity of a polymer composite, the relative permittivity (dielectric constant) can also be enhanced by increasing the volume fraction of liquid metal inclusions, regardless of the size of the inclusions.^[22,111] However, enhancing the dielectric constant to desirable values often requires high liquid metal loading (>50 vol.%), which can result in a drastic loss of material integrity and sometimes percolation.^[69,81,112] The combination of both solid and liquid metal fillers can result in optimized dielectric permittivity with decreased breakdown strength, while still possessing rubber-like compliance and elasticity. In Hu et al.,^[81] eGaIn and polydopamine (PDA)-coated graphene oxide flakes were used in combination in a PDMS matrix to yield a composite with a high dielectric constant (≈10–57), a low dissipation factor (≈0.01), and rubber-like compliance and elasticity. Bury and Kohl^[69] also found that by combining both Galinstan and Fe rigid fillers in a PDMS matrix, permittivity, and loss behavior could be enhanced while maintaining mechanical integrity. Furthermore, the ratio of Fe and Galinstan could be optimized for a specific sensing application, where both mechani-

cal and electrical properties could be precisely adjusted to yield highly stretchable and responsive dielectric materials for use in stretchable electronics and soft robotics.

Self-healing technologies have been extensively demonstrated for the recovery of mechanically damaged parts,^[44,47] but can also be applied to maintaining electrical conductivity.^[73,93,113,114] Electrical self-healing enables the healing and recovery of electrical conductivity in a composite structure after damage. Prior works have shown that liquid metal encapsulated in solid shells can be incorporated into a matrix, and when damaged, will rupture and flow to restore the conductive pathways.^[113,114] The combination of both solid and liquid metal inclusions can enable reversible electrical self-healing. For example, in Park et al.,^[93] Ni flakes and eGaIn were added to a carboxylated polyurethane (CPU) matrix. CPU polymer is engineered to self-heal, and with just eGaIn, can restore electrical conductivity post-damage. However, the eGaIn would eventually leak out of the composite over time, preventing reversible self-healing. The addition of the Ni flakes enables reversible self-healing, as the Ni acts as an anchor for the eGaIn, promoting optimal adhesion between the eGaIn and CPU to prevent leaking over time (Figure 2D). In Ding et al.,^[73] CNTs and gallium liquid metal were directly mixed into a PDMS-polyurethane (PU) blend. The PDMS-PU blend possessed natural self-healing properties, and when coupled with the synergistic electrical properties of both the CNTs and liquid metal, could recover full electrical conductivity when damaged.

2.3. Magnetic Properties

Magnetorheological elastomers (MREs) are magneto-responsive due to the inclusion of magnetic particles within the elastomer matrix.^[115–118] Typically, MREs are synthesized by dispersing solid magneto-responsive fillers, such as ferromagnetic Fe,^[119–121] Ni,^[122–124] or NdFeB^[125–127] particles, in a polymer matrix prior to curing in the presence or absence of a magnetic field. Based on the curing conditions, loading concentration, and type of magnetic particle used, MREs may possess anisotropic physical properties, which can enable field-dependant mechanical or physical properties.^[115,118,128,129] However, due to the solid nature of most magnetic fillers, MREs are often very stiff and tough, with little compliance or stretchability.^[130,131]

Integration of liquid inclusions into MREs can yield composites with not only retained magnetic properties but also enhanced or introduced mechanical and thermal functionalities. Most magneto-responsive LM + x composites make use of either carbonyl Fe^[40,71–73] or NdFeB^[65–67] particles due to their optimal ferromagnetic properties. Ni particles have been used in MREs^[91] but at a lower frequency because the magnetic permeability of Ni is relatively low compared to Fe and NdFeB.^[122] In one example, Zhang et al.^[65] used a NdFeB-liquid metal-PDMS composite to create a miniature, untethered, magnetic robot with dual-energy transmission mode capabilities, which locomotes in response to a low-frequency magnetic field waveform. When subjected to a fast-changing magnetic field, the robot is able to generate enough current to power an LED light. In another example, Guan et al.^[67] used the same materials (NdFeB-eGaIn-PDMS) to synthesize a biomimetic soft inchworm with magneto-responsivity (Figure 2E). The inclusion of both rigid

NdFeB with liquid eGaIn yielded enhanced mechanical properties often seen in liquid metal composites, such as higher flexibility and cross-linking density, decreased swelling, and enhanced tear resistance.^[67]

A unique property that arises from liquid metal + ferromagnetic particle composites is that the electrical conductivity can be tuned by controlling the direction and strength of a magnetic field generated by an electromagnet.^[40,71,72] The magnetic particles in a LM + x composite tend to align in the direction of the magnetic field, which reduces the spacing between the conductive particles. As a result, when the material is subjected to a magnetic field perpendicular to the resistance measurement direction, the electrical resistance decreases. By monitoring the change in resistance, MREs with liquid metal can be used as sensors to measure magnetic flux density and pressures.^[40]

2.4. Thermal Properties

Efficient thermal management is essential for electronic devices, and in the case of wearable computing devices and soft robots, stretchability and deformability are demanded as well. Dispersing high contents of rigid inclusions can enhance thermal conductivity in polymer composite materials but also results in reduced stretchability.^[132–134] Liquid metals exhibit excellent thermal conductivity (relative to other liquid alternatives, such as water, ionic liquids, and hydrocarbons^[135]), in addition to superior electrical properties, and can be dispersed into polymer composites to enhance thermal conductivity while maintaining mechanical compliance.^[30,136] For example, Bartlett et al.^[30] reported a liquid metal elastomer composite with unprecedented metal-like thermal conductivity in a highly stretchable ($\epsilon > 600\%$) state. However, composites containing only liquid metal inclusions at high loading concentrations exhibit low compliance and leakage, thus preventing reliability.

If solid inclusions with high thermal conductivities such as Fe,^[40,68,71] graphite,^[31,77] graphene,^[78–80] Ag,^[68,82,83,90] Ni,^[40,68] or Cu^[68,95,97] are also added to the elastomer, in addition to liquid metal, the thermal conductivity of the multiphase composite will increase relative to the liquid metal-only composite at the same loading percentage. However, the maximum possible volume fraction of the inclusions decreases when rigid inclusions are involved, due to the stiffness of the rigid inclusions, which prevents mixing and uniform formation of a multiphase composite. Therefore, the addition of solid fillers can also reduce the highest achievable thermal conductivity.^[68,137]

Thermal interface materials (TIMs), which are used for the thermal management of high heat flux devices, are required to possess high thermal conductivity with low Young's modulus. However, these two properties typically oppose one another.^[97,138] Zhang et al.^[97] proposed a LM + x composite mixture, wherein a co-doped TIM consisting of liquid metal and Cu in a silicone matrix yielded a thermal conductivity of 3.94 WmK⁻¹ and an elastic modulus of 699 kPa. The performance of this specific TIM was better in comparison to that of the single-phase TIMs, due to the synergistic effects of the highly thermally conductive Cu and the liquid metal fillers, which have very little impact on the mechanical properties of the matrix material. In Sargolzaeiaval et al.,^[78] eGaIn and graphene nanoplatelets (GNPs) in a PDMS matrix

worked together to increase the thermal conductivity of the composite. The affinity between the eGaIn and the GNPs created more paths for phonon transport without increasing the density of the barriers. The thermal conductivity correspondingly increased, as conductive paths formed not only through the GNPs and eGaIn droplets but also through the eGaIn islands that aggregated on the surface of the GNPs. Furthermore, the low loading of rigid GNP filler (<2.2 wt.%) into the composite made it possible to possess high thermal conductivities without substantially impacting the material's flexibility.

Since liquid metals are often denser than the polymer matrices they are embedded in, they tend to settle during curing and prevent uniform heat transfer throughout the bulk composite. However, in some instances, the incorporation of both liquid metal and magneto-responsive particles can aid in introducing multifunctionalities and enhancing the thermal conductivity of a material, promoting a more uniform distribution of heat. For example, in Li et al.,^[71] PDMS and carbonyl Fe particles were mixed with a liquid metal to form a multiphase composite. The thermal conductivity of just the liquid metal-PDMS composite was 0.371 WmK⁻¹, but increased to 0.440 WmK⁻¹ with the addition of the carbonyl Fe particles. The thermal conductivity is enhanced by the addition of carbonyl Fe because the particles form distributed chains in the PDMS matrix when subject to a magnetic field while curing, as shown in Figure 2F, increasing more uniform distribution of thermally conductive particles throughout the matrix. In Yun et al.,^[40] irregularly shaped Ni particles with surface spikes were integrated into a liquid metal-PDMS matrix. Due to the irregular surface area of the Ni particles, more contacts were formed between the particles and liquid metal, enhancing the thermal conductivity of the composite. Furthermore, because the Ni particles exhibit ferromagnetic properties, the enhanced thermal conductivity could be coupled with the magneto-active properties to achieve an intelligent magneto-responsive heating pad.

We note that in the vast majority of LM + x composites, a polymer typically serves as the matrix material encasing both the liquid and solid filler. Here, we highlight some inverted instances that continue to meet our definition of LM + x composites, where the liquid metal serves as the matrix material and hosts multi-material fillers. For example, in Lu et al.,^[66] NdFeB particles are coated with Ag before being incorporated into an eGaIn matrix. Due to the corrosive behavior of gallium-based materials, the Ag acted as a protective barrier to preserve the NdFeB and its inherent magnetic properties. Furthermore, by using a composite material, rather than pure eGaIn, dynamic leakage-free properties were achieved via enhanced viscosity, while retaining excellent heat-storage performance, good thermal stability, low thermal resistance, and high thermal conductivity. In Zhang et al.,^[96] polyphenol-coated Cu particles were dispersed in an eGaIn matrix to yield effective thermal management components for CPU chips, as demonstrated in Figure 2G. Since eGaIn has excellent thermal dissipation properties but low viscosity, the polyphenol-coated Cu particles enhanced the flow properties to prevent surface spreading. Furthermore, the polyphenol-based supramolecular networks served as an effective barrier between the Cu and eGaIn, reducing the alloying interactions and preventing the formation of intermetallic compounds, effectively enhancing the stability of the composite.

3. Materials and Processing

In this section, we review a variety of synthesis techniques for LM + x composites. For completeness, we focus not only on the synthesis of existing LM + x composites, but also on processing methods using liquid metals (absent of x) to comment on future opportunities for the fabrication of LM + x composites.

3.1. Liquid Metal Emulsions

In most cases, the fabrication process of a LM + x composite begins with the preparation of an emulsion, where the uncured polymer matrix is the continuous phase and the liquid metal is the dispersed phase. Thereafter, other fillers can be incorporated prior to polymerization (curing) of the continuous phase to obtain a solid structure containing the encapsulated liquid metal and solid components. Several emulsion processes exist to achieve the mixture of two or more immiscible or partially miscible liquid phases.^[139,140] Mechanical shear is utilized in the emulsification process to break the large particles of the dispersed phase into smaller polydispersed particles distributed throughout the continuous phase. The shear force required for breaking up the dispersed phase can be provided by manual stirring, automated shear homogenization, sonication, or application of acoustic waves.^[141,142] Phase separation is another emulsification method for creating liquid inclusions in a mixture of two partially or entirely miscible fluids. In the phase separation method, the miscibility in a saturated mixture of fluids can be reduced by applying an external stimulus to form droplets in the mixture.^[143]

In the emulsification process, there is a critical capillary number, $Ca = \frac{\tau}{2\sigma/d}$, below which the droplet dispersion is suppressed with surface tension, where τ , σ , and d are shear stress, surface energy, and droplet diameter, respectively. Shear stress obtained from the mechanical agitation causes spherical to ellipsoidal shape deformation in the droplets of the distributed phase, breaking them up into smaller particles, while surface tension opposes this shape deformation.^[144] The emulsification process also depends on the viscosity of the fluids; the viscosity ratio of the dispersed phase to the continuous phase controls the ability of a droplet to split in the continuous phase. At a fixed capillary number, droplet breakups happen if the viscosity ratio is within a specific range of low and high bounds.^[145] In other words, higher capillary numbers are required for mixtures with very low or very high viscosity ratios, which corresponds to higher applied shear stress.

Using a third component as an emulsifying agent is sometimes necessary or useful to facilitate the emulsification process and stability of the emulsion. There are different stabilizing mechanisms for emulsions depending on the system, however, two methods are most commonly used: 1) decreasing interfacial energy, or using surfactants as an emulsifying agent to reduce the interfacial tension generated between the dispersed phase and the continuous phase; and 2) mechanical protection (Pickering emulsion; discussed further in Section 3.3), or incorporating solid particles into the emulsion to be adsorbed and trapped at the interfaces of the dispersed and continuous phases, creating a mechanically strong film to prevent droplet coalescence. When using a surfactant as an emulsifier, the phase in which

the surfactant is more soluble becomes the continuous phase (Brancroft's rule).^[146] Therefore, if the surfactant is not carefully chosen, the emulsion could invert and the intended dispersed phase could emerge as the continuous phase. Surfactants to aid in the emulsification of liquid metals have been well studied, as liquid metals possess a notably high surface tension and are thus difficult to incorporate into different matrix materials. For example, Handschuch-Wang et al.^[147] investigated the effects of a variety of surfactants, such as Tween-80 and sodium dodecyl sulfate, on gallium-based liquid metals, with the goal of preventing droplet coalescence. Different surfactants were found to successfully adsorb onto the surface of the liquid metal droplets based on the chemical environments, preventing liquid metal droplets from agglomerating. Sometimes, dispersants can also be added to aid in the formation of a stable, yet emulsifier or surfactant-free, emulsion. For example, both Park et al.^[93] and Wang et al.^[85] utilized acrylic acid as a dispersant to evenly distribute filler flakes and eGaIn in a polymer network.

3.2. Sequence of Material Incorporation

The literature on multiphase composites containing distinct solid and liquid metal inclusions indicates that the sequence in which the different inclusions are incorporated into the continuous phase plays a vital role in the formation of inclusions and the bulk properties of the resulting composite.^[137] For example, Bilodeau et al.^[31] developed a composite using silicone elastomer as the continuous phase, and liquid metal and solid expanded intercalated graphite (EIG) flakes as the dispersed phases. The liquid metal and silicone elastomer were mixed first, thus breaking up the liquid inclusions into appropriate sizes via shear mixing. Subsequently, EIG suspended in a carrier solvent of cyclohexane was added to the mixture. However, if the EIG had been added to the silicone elastomer first, the viscosity of the mixture would have dropped dramatically due to the incorporation of the solvent, preventing the appropriate breakup of the liquid metal droplets into microscale inclusions.

In some works, the solid filler is introduced into the external matrix prior to liquid metal incorporation.^[75,86–88] In Lopes et al.,^[87] styrene-isoprene block copolymer (SIS) dissolved in toluene was first mixed with Ag flakes to disperse the rigid fillers. Once evenly dispersed, the eGaIn liquid metal was thoroughly mixed into the composite to form a biphasic elastomer ink for stretchable electronics. Interestingly, when the eGaIn was incorporated into the SIS-Ag mixture, the composite yielded not only eGaIn droplets with a gallium oxide shell and Ag flakes in an SIS matrix, but also AgIn₂ microparticles on the surface of the oxide-coated eGaIn droplets. In another work, Yun et al.^[40] placed PDMS, Fe powder, and eGaIn into a container in the sequence stated and shear mixed them to fabricate a composite with distinct dispersed inclusions of Fe particulates and LM inclusions in the bulk PDMS matrix, as shown in **Figure 3A**. In Zhang et al.^[70] eGaIn and solid fillers consisting of either iron or nickel were directly mixed into pre-cure silicones in a one-pot emulsion process to form a uniform stretchable conductive composite, suggesting that simultaneous mixing may achieve similar outcomes to pre-mixing the solid filler and matrix before adding liquid metal in some cases.

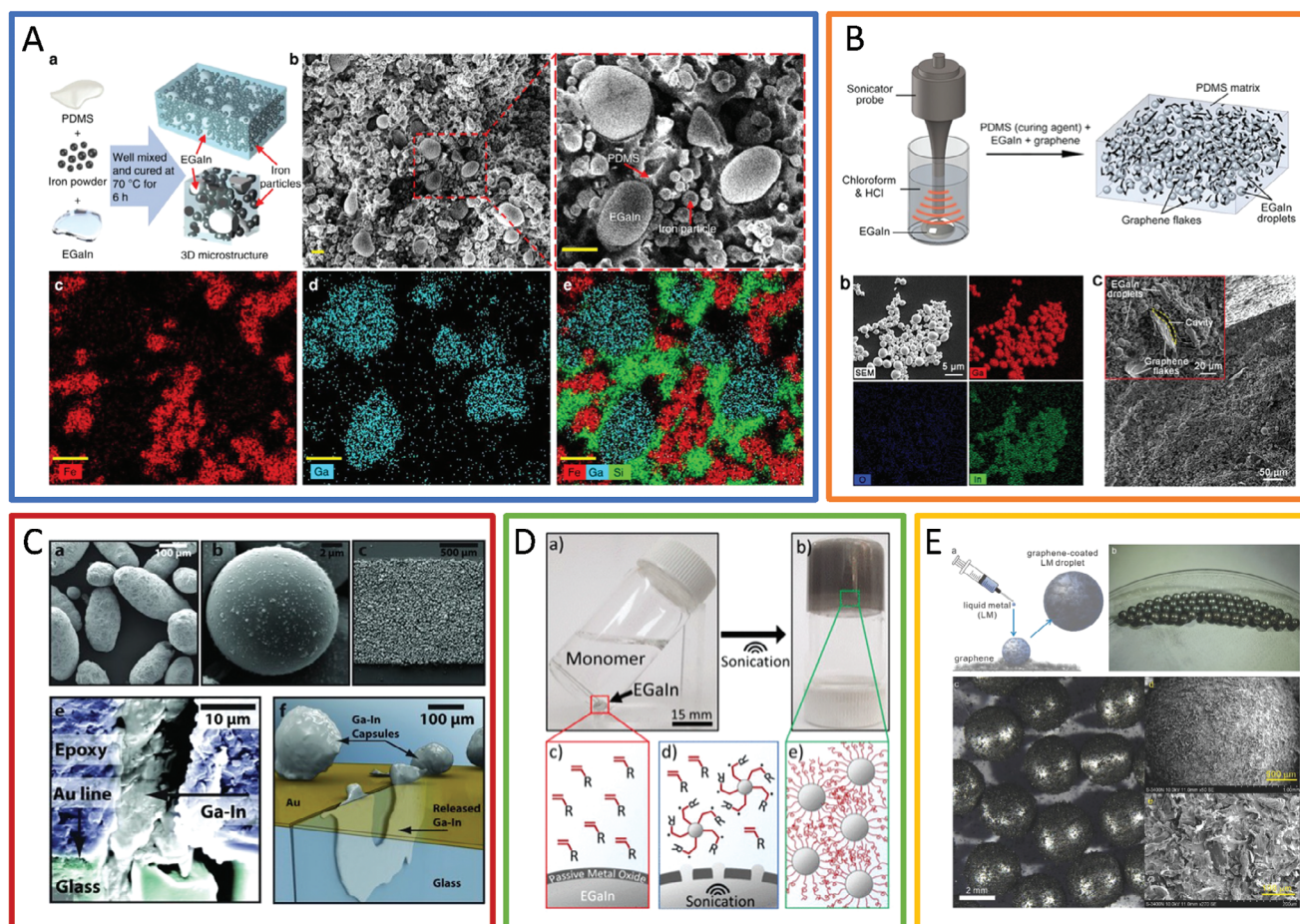


Figure 3. Materials and processing methods for LM + x composites. A) Schematic and scanning electron microscopy (SEM) images with energy dispersive X-ray spectroscopy (EDS) elemental mappings of a LM + x composite. Reproduced with permission.^[40] Copyright 2019, Springer Nature. B) Synthesis process of LM nanodroplets using sonication techniques, which are then collected and incorporated into an elastomeric matrix with additional filler. SEM images with EDS elemental mappings are shown to exhibit the dispersion of the fillers in the elastomeric matrix. Reproduced with permission.^[80] Copyright 2019, Wiley-VCH. C) SEM images of LM encapsulated in a polymer shell using an in situ polymerization process. When embedded in an epoxy matrix and fractured, the cross-sectional SEM image shows the location of the damaged area and liquid metal release (denoted as Ga-In). Additional micro-CT data, with a schematic superimposed, shows the LM-encapsulated microcapsules and their release of liquid metal into the crack plane of a healed specimen. Reproduced with permission.^[113] Copyright 2012, Wiley-VCH. D) Images of an emulsion of LM and a monomer pre- and post-sonication, with a schematic showing the resultant Pickering emulsion formed post-sonication, where organophilic particles stabilize the surface of eGaIn particles. Reproduced with permission.^[148] Copyright 2019, American Chemical Society. E) Schematic of the synthesis process of graphene-coated liquid metal droplets. Optical microscopy and SEM images of the particles show the graphene is evenly dispersed throughout the surface of the eGaIn droplets. Reproduced with permission.^[149] Copyright 2018, Wiley-VCH.

Finally, some works demonstrate that mixing liquid metal with solid fillers (such as metallic particles or flakes) prior to addition to the matrix can aid in the formation of a more uniform composite material with enhanced properties. For example, in Li et al.,^[77] graphite flakes and liquid metal were mixed thoroughly prior to addition into a silicone rubber matrix to yield liquid metal-coated graphite flakes. Both the liquid metal-coated graphite flakes and individual liquid metal droplets dispersed throughout the matrix work synergistically to form a thermally conductive pathway, which is not present in composites of the same composition but without the pre-mixing step. Uppal et al.^[82] showed that when pre-mixing Ag flakes with liquid metal prior to incorporating in silicone oil, which is much less viscous than that of the pre-cure silicone used in Li et al.,^[77] thermal properties were not enhanced

because the filler and liquid metal clumped more frequently. Furthermore, they showed that as the viscosity of the silicone oil increased, the clumping between the solid filler and liquid metal decreased and dispersion increased, which agrees with Li et al.^[77] Tutika et al.^[68] also showed that if solid metal particles (such as Fe or Cu) are mixed with eGaIn prior to shear mixing with silicone elastomer, the liquid metal encapsulates most of the solid particles. This encapsulation of solid particles is likely due to the formation of a gallium-oxide coating around them, which increases the affinity between the particles and eGaIn. Related, Kanetkar et al.^[150] found that pre-mixing solid particles with liquid metal led to air pocket formation, which could negatively impact the bulk composite's thermal conductivity or positively impact density.^[151]

3.3. Liquid Metal Core or Shell Capsules

While liquid metal and other fillers are often embedded into soft matrices via simpler mixing and emulsion processes, these fillers can also be introduced by pre-synthesizing capsules. By fabricating liquid metal capsules prior to addition into a matrix, one may prevent the coalescence of liquid metal droplets in the composite, enable a higher degree of control over the size and morphology of the droplets, and potentially amplify desirable properties.

Gallium-based liquid metal emulsified in a solvent may itself be considered to form core-shell capsules, due to the inherent formation of stabilizing gallium oxide at the surface of each droplet.^[26,152–159] Saborio et al.^[80] synthesized liquid metal capsules by sonicating a mixture of bulk eGaIn in chloroform to break up the liquid metal into droplets, with gallium oxide enclosing the eGaIn particles. Thereafter, the eGaIn capsules and graphene were dispersed in a silicone matrix to yield flexible and stretchable electrically conductive composites (Figure 3B). For a higher degree of control over the size and morphology of the liquid metal suspensions, prior works have also employed stabilizers.^[156,157,160] In Lear et al.,^[156] thiols were added to a mixture of eGaIn and ethanol, with the thiolated emulsion yielding smaller and more monodisperse liquid metal capsules. Finally, microfluidic techniques can also be used to generate monodisperse droplets of liquid metal.^[161,162] Lin et al.^[163] utilized a capillary-based microfluidic approach to synthesize liquid metal microspheres with excellent electrical conductivity and photothermal properties. By modulating the continuous medium in which the liquid metal capsules were synthesized, one can change the size of the synthesized liquid metal spheres. For an extensive review of the intersection between microfluidic techniques and liquid metals, we refer the reader to Zhu et al.^[13]

Other existing processes that can be used to synthesize capsules include interfacial polymerization,^[164–171] in situ polymerization,^[113,114,172–176] and Pickering emulsions.^[177–184] Interfacial polymerization and in situ polymerization techniques are both frequently used to synthesize single core-shell architectures because these methods typically optimize the ratio of core liquid to shell material to maximize the encapsulation of liquid, and some reactions involve a hybrid of both techniques.^[185] In a relevant example of in situ polymerization, Blaiszik et al.^[113] encapsulated eGaIn in a polymeric shell using an in-situ urea-formaldehyde micro-encapsulation technique. The in situ process yielded ellipsoidal capsules with major-axis diameters ranging from 3–200 μm . Thereafter, the liquid metal capsules were incorporated into an epoxy matrix, and upon mechanical damage to the cured matrix, the liquid metal capsules would fracture, enabling the flow of the liquid metal (Figure 3C). While formaldehyde-based in situ polymerization is frequently employed in synthesizing microcapsules, we note that safety concerns associated with formaldehyde,^[186] especially for wearable and biological applications, have motivated the synthesis of melamine-urea microcapsules via interfacial polymerization without the use of formaldehyde.^[187]

In a work employing Pickering emulsions, liquid metal particles were utilized as the Pickering stabilizer, where eGaIn particles self-organized on a porous surface during phase separation to form conductive pathways when mechanically sintered.^[188] Alternatively, the liquid metal can be stabilized by Pickering sta-

bilizers, such as organophilic particles, which can enable stable liquid metal emulsification in a hydrogel matrix,^[148] as shown in Figure 3D. Finally, while not strictly a Pickering emulsion, Chen et al.^[149] coated liquid metal droplets by dropping them into a beaker of graphene sheets and rolling them in the beaker until the droplets were sufficiently coated (Figure 3E), which represents a system of smaller functional particles coating the surface of liquid metal droplets.

In the context of LM + x composites, some works synthesize capsules with solid 'x' filler cores that are coated with liquid metal shells before mixing into a matrix.^[91,95] For example, in He et al.,^[189] polypropylene foam particles were coated with liquid metal by stirring both materials together. The process yielded foam particles with a liquid metal coating of approximately 50 μm . In Hoang et al.,^[91] Ni particles were first coated with eGaIn by mixing both components. Thereafter, the eGaIn-coated Ni particles were dispersed into a silicone matrix. Sometimes, to enhance the wettability between the liquid metal and the solid filler material, the filler can be surface-functionalized. In Chen et al.,^[95] Cu particles were first surface-functionalized with silanes prior to coating with eGaIn to promote wetting and uniform coating. In other cases, the rigid fillers can be coated with a polymer prior to being mixed into a liquid metal matrix. For example, in Zhang et al.,^[96] Cu particles were coated with tannic acid, which is a polyphenol polymer, prior to mixing into an eGaIn matrix. The polyphenol polymer coating prevented alloying interactions between the eGaIn and Cu particles and delayed the formation of intermetallic compounds, which proved favorable for thermal applications.

3.4. Inclusion Settling and Composite Homogeneity

Settling of the inclusions may impact the homogeneity of all LM + x composite formulations. Liquid metals typically possess a high density, on the order of seven times that of the elastomers they are frequently encapsulated in [190]. Because of the large difference in densities between the liquid metal and the matrix, settling of the dense liquid metals during curing often occurs, leading to non-uniform samples. The settling phenomena found in liquid metal composites can often have detrimental effects, causing a lowered dielectric constant along with lowered electrical and thermal conductivity. Several works have aimed to mitigate the segregation and settling of liquid metals in elastomer composites.^[190,191] One approach is to mix low-density materials, such as hollow glass microspheres, with the liquid metal prior to its addition into an elastomer matrix.^[191] Mixing up to 50 vol.% of the low-density microspheres into the liquid metal can reduce the density to almost half of the neat liquid metal, which prevents settling during curing. In another approach, Xue et al.^[190] mixed pre-synthesized PDMS beads with liquid metal and pre-cure PDMS to prevent settling and segregation. The PDMS beads and liquid metal inclusions work synergistically to jam and prevent the inclusions from settling.

4. Theory and Modeling

In this section, we review relevant literature that contributes to the predictive modeling of LM + x composites. As LM + x

multiphase composites contain both liquid and solid inclusions, we begin by discussing modeling approaches for composites containing each distinct filler phase before reviewing combinatorial approaches.

4.1. Composites with Solid Inclusions

There are several theoretical models to estimate the effect of solid inclusions on the mechanical properties of composites. Mechanical properties of the inclusions and their volume fraction are the governing parameters in most of these models, however, the geometry of the fillers and their packing fraction have also been considered in some advanced models. The simplest way to predict the mechanical properties of a composite such as elastic modulus, density, Poisson's ratio, and strength is through series and parallel models based on the rule of mixtures. For elastic modulus, the series and parallel models consider that the fillers and the matrix are under uniform tension and deformation, which is a simplification. In continuum mechanics, Eshelby's theory^[192] of solid composites expresses the responses of ellipsoidal inclusions in composites to applied stresses, and the stiffness of solid composites with low concentrations of inclusions can be predicted. Eshelby's theory has also been extended to higher concentrations of inclusions when the strain fields of neighboring inclusions affect each other.^[193,194] On the other hand, the Halpin-Tsai empirical model equations have been used extensively to predict the properties of composites reinforced with short fibers considering the aspect ratio of the fillers. The Halpin-Tsai model reduces to the parallel and series models when the empirical parameter defined in it becomes very large or very small, respectively. The Halpin-Tsai equations take a more intricate form when the fibers are randomly oriented in the composite matrix.^[195]

4.2. Composites with Liquid Metal Inclusions

For composites with liquid inclusions, as predicted by Eshelby's classic theory, the stiffness of a composite should decrease by incorporating liquid inclusions, as the elastic modulus of liquid inclusions is zero. This theory has been shown to be effective for composites containing inclusions with radius $R > \gamma/E$, where γ is the surface tension and E is the elastic modulus of the matrix.^[196] Eshelby's theory further predicts that the elastic modulus of the composite E_c with volume fraction ϕ of liquid inclusions is $E_c = \frac{E}{1+5\phi/3}$. However, this conventional composite theory does not account for surface tension at the liquid–solid interface. $L \equiv \gamma/E$ is the elastocapillary length below which the surface tension at the liquid–solid interface can significantly oppose the deformation of the bulk composite, and the conventional composite theories fail to predict the elastic moduli of the composites with liquid inclusions at that scale (Figure 4A).^[197] The reinforcing effect of the liquid–solid interface has been shown for single liquid-filled microcapsules^[35] and also dispersed liquid inclusions in elastomers.^[198–203] Style et al.^[196] postulated that to include the surface tension effect in the Eshelby equation for predicting composite elastic modulus

E_c , the liquid inclusions can be considered as soft elastic inclusions:

$$E_c = E \frac{1 + \frac{2}{3} \frac{E_i}{E}}{\left(\frac{2}{3} - \frac{5\phi}{3}\right) \frac{E_i}{E} + \left(1 + \frac{5\phi}{3}\right)} \quad (1)$$

where E_i is the effective elastic modulus obtained from the properties of the dispersed and continuous phases as follows:

$$E_i = E \frac{24 \frac{\gamma}{ER}}{10 + 9 \frac{\gamma}{ER}} \quad (2)$$

This equivalent elastic modulus can also be replaced in other established composite theories such as the Mori-Tanaka method^[194] to account for surface tension forces in structures with higher contents of liquid inclusions since the Eshelby theory just covers dilute composites.

Other force interactions at the liquid–solid interfaces in composites, such as cross-linking at the interface of silicone-ionic liquid^[196] or oxide skin at the interface of eGaIn drops encapsulated in elastomer,^[198] can also increase the effective elastic modulus of the soft inclusions beyond the limit predicted by Equation (2). Bartlett et al.^[198] reported that by dispersing eGaIn in silicone elastomer, the value obtained from Equation (2) was $E_i = 129$ kPa, but they found agreement between their experimental data and Equation (1) when $E_i = 320$ kPa (Figure 4B). The difference in the elastic modulus of inclusions could be attributed to the presence of stiff oxide skin around the liquid metal inclusions, as studied by Lear et al.^[156] and Buckner et al.,^[202] and also the interaction between adjacent inclusions, which was not predicted in Eshelby's theory.

4.3. Composites with Liquid Metal + x Inclusions

To model the mechanical properties of composites containing both solid and liquid inclusions, Mohammadi Nasab et al.^[205] proposed that one can compute the composite property considering just one of the inclusions in the continuous phase first, and then use that as the property of the continuous phase when considering the second filler. Tutika et al.^[68] proposed a related approach to predict the thermal conductivity in multiphase composites using a variation of the Cheng-Vachon^[206] and Bruggeman^[207] models, wherein the LM suspension in an elastomer is considered to be the continuous phase and Fe particles are the discontinuous phase. Thus, the authors predict the multiphase composite's thermal conductivity using a two-phase model (Figure 4C). Phan-Thien et al.^[208] took the approach of a “differential scheme,” where the multiphase composite is sequentially built up through a series of incremental additions until the final volume fractions are reached. During each sequential modeling step, the intermediate composite properties are used as the continuous phase and the incrementally added compounds as the dispersed phase, thus achieving a discretized implementation of the two-phase model. In general, such sequential, embedded, or discretized two-phase models offer enough simplicity and explicitness to make them an attractive approach for the thermal and mechanical modeling of LM + x composites.

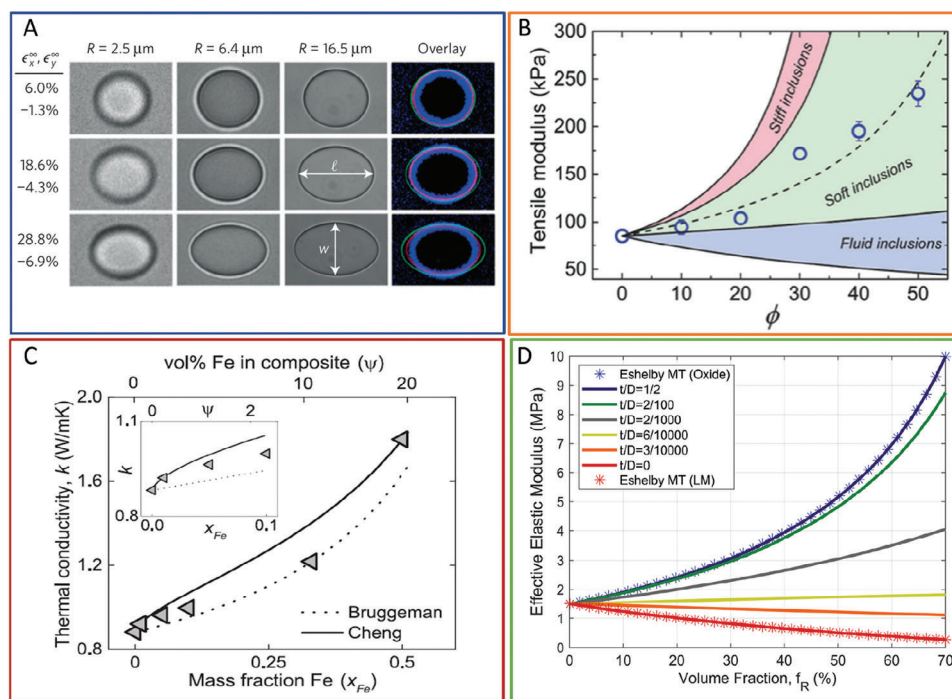


Figure 4. Predictive modeling of LM + x composites. A) Images of ionic-liquid droplets with different radii in a soft matrix with $E = 1.7$ kPa, under different uniaxial stress in the x direction. Smaller droplets show less deformation under the same applied strain. Reproduced with permission.^[196] Copyright 2015, Springer Nature. B) Tensile modulus versus volume fraction (ϕ) of liquid metal particles in a silicone elastomer. Different regimes of inclusion stiffness are found using Equation (1), and the dashed line is the prediction from Equation (1) for liquid metal inclusions. Reproduced with permission.^[198] Copyright 2016, Wiley-VCH. C) Thermal conductivity as a function of Fe mass fraction in a LM + Fe composite, in comparison to Bruggeman and Cheng-Vachon model predictions. The loading of LM is 30 vol.%. Reproduced with permission.^[68] Copyright 2018, Wiley-VCH. D) Effective elastic modulus predicted by two-level double inclusion (DI) model for different volume fractions and shell thickness to diameter ratio (t/D) of LM inclusions in an elastomer. Comparisons to Eshelby's model are shown using the properties of gallium-oxide and neat LM. Reproduced with permission.^[204] Copyright 2021, Elsevier.

Other approaches in the literature include a double inclusion model capable of predicting the properties of polymer composites with core-shell liquid metal droplets, proposed by Chiew and Malakooti.^[204] In this double inclusion model (Figure 4D), the elasticity of the LM inclusions is actively tuned according to the relative shell thickness of gallium oxide surrounding each inclusion, where it is known that as the size of droplets decreases the oxide shell becomes more mechanically dominant.^[156,202] Bury and Koh^[69] employed a microcapacitor model in their work to study the electrical behavior of multiphase composites. Therein, the composite is modeled as a network of randomly distributed microcapacitors in the host matrix. Finally, Chen et al.^[95] modeled the thermal properties of multiphase composites using an augmented Agari's model,^[209] which outputs a composite's thermal conductivity as a function of the filler properties. To conclude this section, we note that theoretical approaches to predicting the behavior of multiphase composites appear limited in the literature, thus positioning the derivation of models for composites containing distinct solid and liquid inclusions as an opportunity for future advancement.

5. Conclusion and Outlook

In this review, we consolidated the literature on multiphase composites containing liquid metal inclusions and other solid (x)

fillers. We view this sub-class of liquid metal-inclusive multiphase composites as increasingly important. Liquid metals have proven to be exciting, intriguing, and useful materials, as evidenced by the number of papers published annually using "liquid metal" as a keyword doubling over the last 10 years (Clarivate, Web of Science). With this explosion of findings on liquid metal properties and potential applications, it is expected that we might seek to improve or otherwise expand the capabilities of other materials and composites by simply adding liquid metal. This is how we arrived at our characterization of multiphase composites containing liquid metal as 'liquid metal + x,' which we view as analogous to the common approach of wrapping artificial intelligence (AI) around arbitrary models or simulations in associated areas (e.g., x = healthcare, medicine, biology, cybersecurity, finance, business, manufacturing, and transportation) to yield previously undiscovered solutions (AI + x). Similarly, here we propose that liquid metal can be integrated into many composite materials with functional fillers (e.g., x = Ag, Cu, Fe, Ni, graphite, graphene, etc.) to yield previously untapped, unparalleled, or multiplied functional properties.

We identify two grand challenges that should be addressed to enable future progress in LM + x composites, pertaining to 1) fabrication and 2) modeling. As discussed herein, the fabrication of LM + x composites, and multiphase composites overall, can be either straightforward or highly complex, depending on the

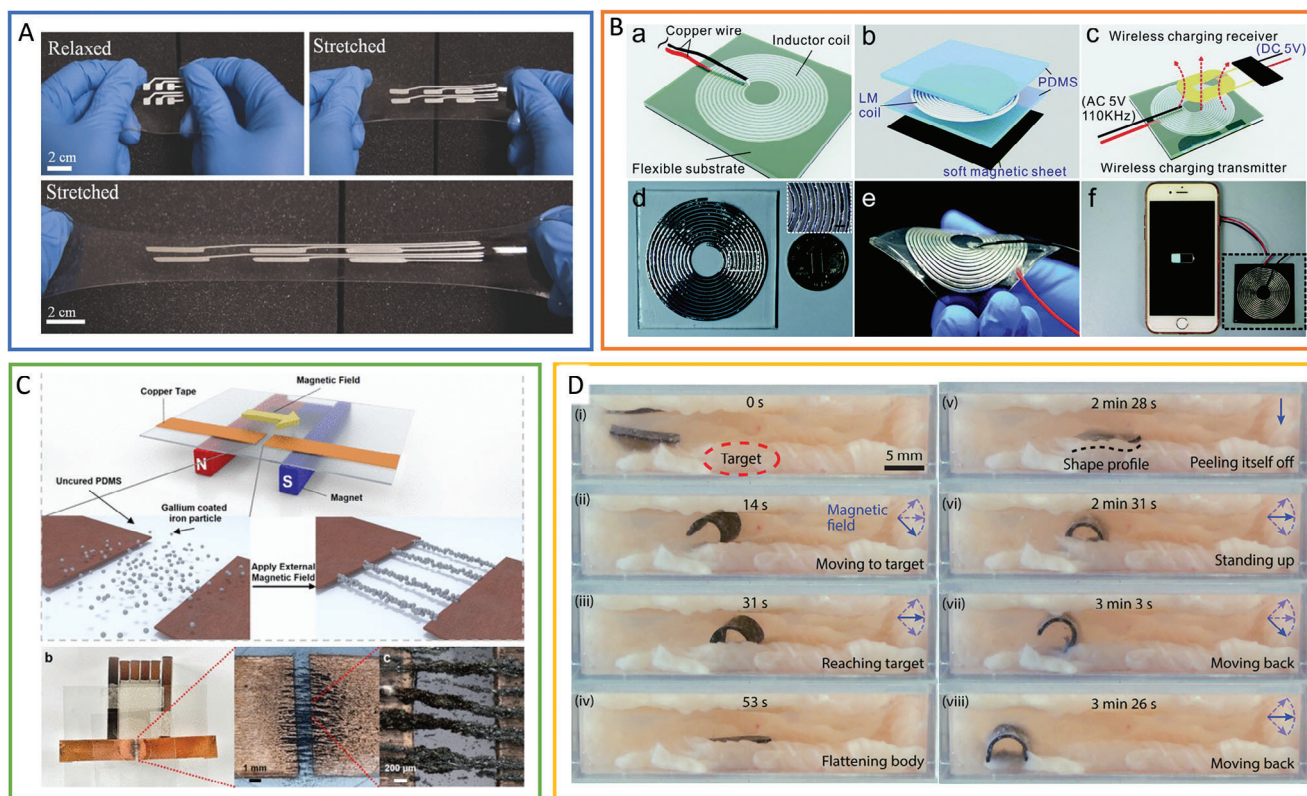


Figure 5. Applications of LM + x composites. A) A stretchable and printable superelastic conductor based on a LM + silver composite. Images show the composite in relaxed and stretched (up to 800%) states. Reproduced with permission.^[85] Copyright 2018, Wiley-VCH. B) Schematic and images of a liquid metal coil for wireless charging via inductive coupling. Images show the flexibility and charging capabilities of the coil. Reproduced with permission.^[212] Copyright 2019, Royal Society of Chemistry. C) Schematic and images of remotely assembled microwires using an external magnetic field. Gallium-coated iron particles align in response to a magnetic field, effectively electrically coupling the two copper tapes together. Reproduced with permission.^[72] Copyright 2022, American Chemical Society. D) Images of an untethered miniature magnetic soft robot locomoting in a tissue-covered chamber. The robot can move to a target region and heat the area, performing localized ablation, in response to a magnetic field. Reproduced with permission.^[65] Copyright 2022, Wiley-VCH.

specific material compatibilities. The literature indicates that successful sample fabrication is sensitive to the sequence in which components are incorporated. Correspondingly, we found works in which i) the liquid metal and matrix should be first mixed before adding a solid filler, ii) the solid filler and matrix should be first mixed before adding the liquid metal inclusions, and iii) the liquid metal and solid fillers should be first mixed before incorporation into the matrix material. Furthermore, while the properties of LM are mostly constant, the properties of x and the matrix may vary, making synthesis processes sensitive to specific material compatibilities and thus difficult to generalize. The study and discovery of guidelines to synthesize LM + x composites will aid the community in the identification of appropriate fabrication processes for increasingly complex and multifunctional composites.

We also found in our literature review that the derivation of accessible predictive models for LM + x composites represents a substantial challenge for the field, and the few models that exist tend to be highly complex and bespoke. This is unsurprising and coupled to the variability in fabrication approaches discussed above. For example, Mohammadi Nasab et al.^[205] proposed a sequential approach—that one could model a single-inclusion composite, and the resulting properties could be input as the contin-

uous phase in the model again with a new dispersed phase—which demands a certain processing order. It is unclear if such a sequential modeling approach would apply to LM + x composites fabricated using simultaneous mixing of all components or otherwise inverted sequencing. Deriving the underpinning mechanistic principles of multiphase composites will enable generalized, predictive models of bulk thermal and mechanical material properties.

Overall, LM + x composites are becoming increasingly common in the literature, and their potential impact spans broad applications including stretchable electronics, wearables, soft robotics, thermal management, and energy harvesting and storage. Many technological advancements toward these applications can still be attained through fabrication and modeling breakthroughs. For example, although highly stretchable conductors have already been achieved by filling elastomers with conductive LM + x inclusions, secure, and effective integration of rigid microelectronics with multilayer flexible circuitry remains a challenge. Such integration challenges could be solved via precise control of the sizes, shapes, and distribution patterns of the LM + x inclusions.^[210] Maturation and generalization of the manufacturing processes used for LM + x composites will enable translation to commercialization.

Exciting products have already been proposed, including ultra-stretchable conductive interconnects^[85,107] (Figure 5A), wearable wireless power transmitters^[211,212] (Figure 5B), remotely assembled circuits^[72] (Figure 5C), and sensors and actuators for soft robots^[65,86] (Figure 5D), and we foresee the continued proliferation of LM + x composites due to their uniquely enhanced, enabled, and multiplied properties.

Acknowledgements

S.E. and A.M.N. contributed equally to this work. S.E. was supported by a NASA Space Technology Graduate Research Fellowship under Grant no. 80NSSC21K1269. A.M.N. was supported by the National Science Foundation (NSF) under Grant no. EFMA-1830870. X.H. and R.K.B. were supported by the NSF under Grant no. IIS-1956027.

Conflict of Interest

The authors declare no conflict of interest.

Keywords

functional composites, gallium, liquid inclusions, multiphase inclusions, solid inclusions

Received: August 11, 2023
Revised: November 10, 2023
Published online:

- [1] S.-Y. Tang, C. Tabor, K. Kalantar-Zadeh, M. D. Dickey, *Annu. Rev. Mater. Res.* **2021**, *51*, 381.
- [2] M. H. Malakooti, N. Kazem, J. Yan, C. Pan, E. J. Markvicka, K. Matyjaszewski, C. Majidi, *Adv. Funct. Mater.* **2019**, *29*, 1906098.
- [3] A. Martin, B. S. Chang, M. Thuo, *ACS Appl. Nano Mater.* **2022**, *5*, 3325.
- [4] S. Chen, R. Zhao, X. Sun, H. Wang, L. Li, J. Liu, *Adv. Healthcare Mater.* **2023**, *12*, 2201924.
- [5] M. D. Dickey, R. C. Chiechi, R. J. Larsen, E. A. Weiss, D. A. Weitz, G. M. Whitesides, *Adv. Funct. Mater.* **2008**, *18*, 1097.
- [6] R. C. Chiechi, E. A. Weiss, M. D. Dickey, G. M. Whitesides, *Angew. Chem., Int. Ed.* **2008**, *47*, 142.
- [7] R. J. Larsen, M. D. Dickey, G. M. Whitesides, D. A. Weitz, *J. Rheol.* **2009**, *53*, 1305.
- [8] Y. Ding, M. Zeng, L. Fu, *Matter* **2020**, *3*, 1477.
- [9] M. R. Khan, C. B. Eaker, E. F. Bowden, M. D. Dickey, *Proc. Natl. Acad. Sci. USA* **2014**, *111*, 14047.
- [10] J. Ma, F. Krisnadi, M. H. Vong, M. Kong, O. M. Awartani, M. D. Dickey, *Adv. Mater.* **2023**, *35*, 2205196.
- [11] S. Zhang, Y. Liu, Q. Fan, C. Zhang, T. Zhou, K. Kalantar-Zadeh, Z. Guo, *Energy Environ. Sci.* **2021**, *14*, 4177.
- [12] J. Yang, W. Cheng, K. Kalantar-Zadeh, *Proc. IEEE* **2019**, *107*, 2168.
- [13] L. Zhu, B. Wang, S. Handschuh-Wang, X. Zhou, *Small* **2020**, *16*, 1903841.
- [14] X. Sun, B. Yuan, L. Sheng, W. Rao, J. Liu, *Appl. Mater. Today* **2020**, *20*, 100722.
- [15] P. Won, S. Jeong, C. Majidi, S. H. Ko, *Iscience* **2021**, *24*, 7.
- [16] Y.-G. Park, G.-Y. Lee, J. Jang, S. M. Yun, E. Kim, J.-U. Park, *Adv. Healthcare Mater.* **2021**, *10*, 2002280.
- [17] K. N. Paracha, A. D. Butt, A. S. Alghamdi, S. A. Babale, P. J. Soh, *Sensors* **2019**, *20*, 177.
- [18] J. L. Melcher, K. S. Elassy, R. C. Ordonez, C. Hayashi, A. T. Ohta, D. Garmire, *Micromachines* **2019**, *10*, 54.
- [19] Y. Tang, C.-H. Huang, K. Nomura, *ACS Nano* **2022**, *16*, 3280.
- [20] M. Zaheer, Y. Cai, A. B. Waqas, S. F. Abbasi, G. Zhu, C. Cong, Z.-J. Qiu, R. Liu, Y. Qin, L. Zheng, et al., *Phys. Status Solidi RRL* **2020**, *14*, 2000050.
- [21] S. Nayak, Y. Li, W. Tay, E. Zamburg, D. Singh, C. Lee, S. J. A. Koh, P. Chia, A. V.-Y. Thean, *Nano Energy* **2019**, *64*, 103912.
- [22] C. Pan, E. J. Markvicka, M. H. Malakooti, J. Yan, L. Hu, K. Matyjaszewski, C. Majidi, *Adv. Mater.* **2019**, *31*, 1900663.
- [23] M. H. Malakooti, M. R. Bockstaller, K. Matyjaszewski, C. Majidi, *Nanoscale Adv.* **2020**, *2*, 2668.
- [24] X. Wang, R. Guo, J. Liu, *Adv. Mater. Technol.* **2019**, *4*, 1800549.
- [25] T. V. Neumann, M. D. Dickey, *Adv. Mater. Technol.* **2020**, *5*, 2000070.
- [26] S. Liu, D. S. Shah, R. Kramer-Bottiglio, *Nat. Mater.* **2021**, *20*, 851.
- [27] M. J. Ford, C. P. Ambulo, T. A. Kent, E. J. Markvicka, C. Pan, J. Malen, T. H. Ware, C. Majidi, *Proc. Natl. Acad. Sci. USA* **2019**, *116*, 21438.
- [28] E. J. Markvicka, M. D. Bartlett, X. Huang, C. Majidi, *Nat. Mater.* **2018**, *17*, 618.
- [29] C. J. Thrasher, Z. J. Farrell, N. J. Morris, C. L. Willey, C. E. Tabor, *Adv. Mater.* **2019**, *31*, 1903864.
- [30] M. D. Bartlett, N. Kazem, M. J. Powell-Palm, X. Huang, W. Sun, J. A. Malen, C. Majidi, *Proc. Natl. Acad. Sci. USA* **2017**, *114*, 2143.
- [31] R. A. Bilodeau, A. M. Nasab, D. S. Shah, R. Kramer-Bottiglio, *Soft Matter* **2020**, *16*, 5827.
- [32] G. Yun, S.-Y. Tang, Q. Zhao, Y. Zhang, H. Lu, D. Yuan, S. Sun, L. Deng, M. D. Dickey, W. Li, *Matter* **2020**, *3*, 824.
- [33] S.-Y. Fu, X.-Q. Feng, B. Lauke, Y.-W. Mai, *Composites, Part B* **2008**, *39*, 933.
- [34] Y. Katoh, Y. Matsuda, W. Ando, M. Matsukage, S. Tasaka, *J. Appl. Polym. Sci.* **2011**, *120*, 1278.
- [35] A. C. Chipara, P. S. Owuor, S. Bhowmick, G. Brunetto, S. S. Asif, M. Chipara, R. Vajtai, J. Lou, D. S. Galvao, C. S. Tiwary, et al., *Adv. Mater. Interfaces* **2017**, *4*, 1600781.
- [36] T. L. Buckner, M. C. Yuen, S. Y. Kim, R. Kramer-Bottiglio, *Adv. Funct. Mater.* **2019**, *29*, 1903368.
- [37] X. Zhang, Y. Pan, L. Shen, Q. Zheng, X. Yi, *J. Appl. Polym. Sci.* **2000**, *77*, 1044.
- [38] X. Zhang, Y. Pan, L. Shen, X. Yi, *J. Appl. Polym. Sci.* **2000**, *77*, 756.
- [39] D. Amoabeng, S. S. Velankar, *Polym. Eng. Sci.* **2018**, *58*, 1010.
- [40] G. Yun, S.-Y. Tang, S. Sun, D. Yuan, Q. Zhao, L. Deng, S. Yan, H. Du, M. D. Dickey, W. Li, *Nat. Commun.* **2019**, *10*, 1300.
- [41] M. Vázquez, A. Hernandez, *Adv. Mater.* **1995**, *7*, 217.
- [42] K. Pietrak, T. S. Wiśniewski, *J. Power Technol.* **2015**, *95*, 1.
- [43] G. Caylı, S. Küsefoğlu, *J. Appl. Polym. Sci.* **2006**, *100*, 832.
- [44] S. R. White, N. R. Sottos, P. H. Geubelle, J. S. Moore, M. R. Kessler, S. Sriram, E. N. Brown, S. Viswanathan, *Nature* **2001**, *409*, 794.
- [45] T. Yin, M. Z. Rong, M. Q. Zhang, G. C. Yang, *Compos. Sci. Technol.* **2007**, *67*, 201.
- [46] D. S. Xiao, Y. C. Yuan, M. Z. Rong, M. Q. Zhang, *Polymer* **2009**, *50*, 2967.
- [47] M. D. Hager, P. Greil, C. Leyens, S. van der Zwaag, U. S. Schubert, *Adv. Mater.* **2010**, *22*, 5424.
- [48] X.-W. Zhang, Y. Pan, Q. Zheng, X.-S. Yi, *J. Appl. Polym. Sci.* **2002**, *86*, 3173.
- [49] H.-J. Song, Z.-Z. Zhang, X.-H. Men, *Composites, Part A* **2008**, *39*, 188.
- [50] K. Friedrich, U. Breuer, *Multifunctionality of polymer composites: challenges and new solutions*, William Andrew, Norwich, NY **2015**.
- [51] H. Wang, Y. Yao, X. Wang, L. Sheng, X.-H. Yang, Y. Cui, P. Zhang, W. Rao, R. Guo, S. Liang, et al., *ACS Omega* **2019**, *4*, 2311.
- [52] R. Dou, Y. Shao, S. Li, B. Yin, M. Yang, *Polymer* **2016**, *83*, 34.
- [53] T. K. Gupta, B. P. Singh, R. B. Mathur, S. R. Dhakate, *Nanoscale* **2014**, *6*, 842.

- [54] S.-Y. Zhang, Q. Zhuang, M. Zhang, H. Wang, Z. Gao, J.-K. Sun, J. Yuan, *Chem. Soc. Rev.* **2020**, *49*, 1726.
- [55] R. W. Style, R. Tutika, J. Y. Kim, M. D. Bartlett, *Adv. Funct. Mater.* **2021**, *31*, 2005804.
- [56] N. Kazem, T. Hellebrekers, C. Majidi, *Adv. Mater.* **2017**, *29*, 1605985.
- [57] S. Chen, H.-Z. Wang, R.-Q. Zhao, W. Rao, J. Liu, *Matter* **2020**, *2*, 1446.
- [58] N. Ochirkhuyag, R. Matsuda, Z. Song, F. Nakamura, T. Endo, H. Ota, *Nanoscale* **2021**, *13*, 2113.
- [59] G. G. Guymon, M. H. Malakooti, *J. Polym. Sci.* **2022**, *60*, 1300.
- [60] Y. Lin, J. Genzer, M. D. Dickey, *Adv. Sci.* **2020**, *7*, 2000192.
- [61] H. Song, T. Kim, S. Kang, H. Jin, K. Lee, H. J. Yoon, *Small* **2020**, *16*, 1903391.
- [62] C. Chiew, M. J. Morris, M. H. Malakooti, *Mater. Adv.* **2021**, *2*, 7799.
- [63] W. Xie, F.-M. Allieux, J. Z. Ou, E. Miyako, S.-Y. Tang, K. Kalantar-Zadeh, *Trends Biotechnol.* **2021**, *39*, 624.
- [64] H. Wang, R. Li, Y. Cao, S. Chen, B. Yuan, X. Zhu, J. Cheng, M. Duan, J. Liu, *Adv. Fiber Mater.* **2022**, *4*, 987.
- [65] J. Zhang, R. H. Soon, Z. Wei, W. Hu, M. Sitti, *Adv. Sci.* **2022**, *9*, 2203730.
- [66] Y. Lu, D. Yu, H. Dong, S. Chen, H. Zhou, L. Wang, Z. Deng, Z. He, J. Liu, *Adv. Funct. Mater.* **2023**, *33*, 2210961.
- [67] Y. Guan, Y. Liu, Q. Wang, H. Geng, T. Cui, Y. Hu, Q. Luo, A. Li, W. Li, Y. Lin, L. Zhang, G. Liu, J. Fan, L. Wu, *Chem. Eng. J.* **2023**, *466*, 142994.
- [68] R. Tutika, S. H. Zhou, R. E. Napolitano, M. D. Bartlett, *Adv. Funct. Mater.* **2018**, *28*, 1804336.
- [69] E. Bury, A. S. Koh, *ACS Appl. Mater. Interfaces* **2022**, *14*, 13678.
- [70] Q. Zhang, G. Yun, B. Zhao, H. Lu, S. Zhang, S.-Y. Tang, W. Li, *Smart Mater. Struct.* **2021**, *30*, 115005.
- [71] W. Li, S. Liu, C. Lou, M. Sang, X. Gong, K. C.-F. Leung, S. Xuan, *Cell Rep. Phys. Sci.* **2023**, *4*, 1.
- [72] S. Kim, S. Kim, K. Hong, M. D. Dickey, S. Park, *ACS Appl. Mater. Interfaces* **2022**, *14*, 37110.
- [73] L. Ding, S. Zhang, Q. Wang, Y. Wang, S. Xuan, X. Gong, D. Zhang, *Compos. Sci. Technol.* **2022**, *223*, 109430.
- [74] Y. Guan, Y. Liu, Q. Li, Y. Shi, H. Li, J. Guo, G. Zhang, C. Liu, W. Li, G. Liu, Z. Liu, *Compos. Struct.* **2022**, *291*, 115653.
- [75] C. Li, H. Chen, L. Zhang, J. Zhong, *AIP Adv.* **2020**, *10*, 10.
- [76] J. Zhang, M. Liu, G. Pearce, Y. Yu, Z. Sha, Y. Zhou, A. C. Yuen, C. Tao, C. Boyer, F. Huang, M. Islam, C. H. Wang, *Compos. Sci. Technol.* **2021**, *201*, 108497.
- [77] A. Li, P. Wang, J.-Y. Li, Z.-Q. Xiong, Y. Huang, *Int. J. Mod. Phys. B* **2022**, *36*, 2250078.
- [78] Y. Sargolzaeiaval, V. P. Ramesh, T. V. Neumann, R. Miles, M. D. Dickey, M. C. Öztürk, *ECS J. Solid State Sci. Technol.* **2019**, *8*, P357.
- [79] Y. Sargolzaeiaval, V. P. Ramesh, T. V. Neumann, V. Misra, D. Vashae, M. D. Dickey, M. C. Öztürk, *Appl. Energy* **2020**, *262*, 114370.
- [80] M. G. Saborio, S. Cai, J. Tang, M. B. Ghasemian, M. Mayyas, J. Han, M. J. Christoe, S. Peng, P. Koshy, D. Esrafilzadeh, R. Jalili, C. H. Wang, K. Kalantar-Zadeh, *Small* **2020**, *16*, 1903753.
- [81] Y. Hu, C. Majidi, *ACS Appl. Mater. Interfaces* **2023**, *5*, 1376.
- [82] A. Uppal, W. Kong, A. Rana, R. Y. Wang, K. Rykaczewski, *ACS Appl. Mater. Interfaces* **2021**, *13*, 43348.
- [83] A. Uppal, W. Kong, A. Rana, J. S. Lee, M. D. Green, K. Rykaczewski, R. Y. Wang, *Adv. Mater. Interfaces* **2023**, *10*, 2201875.
- [84] Z. Liu, S. Chen, G. Zhang, H. Shi, X. Chen, W. Shi, L. Liu, *Adv. Mater. Interfaces* **2022**, *9*, 2102121.
- [85] J. Wang, G. Cai, S. Li, D. Gao, J. Xiong, P. S. Lee, *Adv. Mater.* **2018**, *30*, 1706157.
- [86] M. Reis Carneiro, C. Majidi, M. Tavakoli, *Adv. Eng. Mater.* **2022**, *24*, 2100953.
- [87] P. A. Lopes, D. F. Fernandes, A. F. Silva, D. G. Marques, A. T. de Almeida, C. Majidi, M. Tavakoli, *ACS Appl. Mater. Interfaces* **2021**, *13*, 14552.
- [88] J. Sgotti Veiga, M. Reis Carneiro, R. Molter, M. Vinciguerra, L. Yao, C. Majidi, M. Tavakoli, *Adv. Mater. Technol.* **2023**, *3*, 2300144.
- [89] A. Hajalilou, A. F. Silva, P. A. Lopes, E. Parvini, C. Majidi, M. Tavakoli, *Adv. Mater. Interfaces* **2022**, *9*, 2101913.
- [90] W. Kong, Z. Wang, N. Casey, M. M. Korah, A. Uppal, M. D. Green, K. Rykaczewski, R. Y. Wang, *Adv. Mater. Interfaces* **2021**, *8*, 2100069.
- [91] T. T. Hoang, P. T. Phan, M. T. Thai, J. Davies, C. C. Nguyen, H.-P. Phan, N. H. Lovell, T. N. Do, *Adv. Intell. Syst.* **2022**, *4*, 2200282.
- [92] A. Hajalilou, E. Parvini, J. P. M. Pereira, P. A. Lopes, A. F. Silva, A. De Almeida, M. Tavakoli, *Adv. Mater. Technol.* **2023**, *8*, 2201621.
- [93] S. Park, G. Thangavel, K. Parida, S. Li, P. S. Lee, *Adv. Mater.* **2019**, *31*, 1805536.
- [94] G. Yun, S.-Y. Tang, H. Lu, T. Cole, S. Sun, J. Shu, J. Zheng, Q. Zhang, S. Zhang, M. D. Dickey, W. Li, *ACS Appl. Polymer Mater.* **2021**, *3*, 5302.
- [95] S. Chen, W. Xing, H. Wang, W. Cheng, Z. Lei, F. Zheng, P. Tao, W. Shang, B. Fu, C. Song, M. D. Dickey, T. Deng, *Chem. Eng. J.* **2022**, *439*, 135674.
- [96] C. Zhang, Y. Tang, T. Guo, Y. Sang, D. Li, X. Wang, O. J. Rojas, J. Guo, *InfoMat* **2023**, e12466.
- [97] X.-D. Zhang, Z.-T. Zhang, H.-Z. Wang, B.-Y. Cao, *ACS Appl. Mater. Interfaces* **2023**, *15*, 35832.
- [98] A. Papon, H. Montes, F. Lequeux, J. Oberdisse, K. Saalwächter, L. Guy, *Soft Matter* **2012**, *8*, 4090.
- [99] J. Cho, M. Joshi, C. Sun, *Compos. Sci. Technol.* **2006**, *66*, 1941.
- [100] G. Gallone, F. Carpi, D. De Rossi, G. Levita, A. Marchetti, *Mater. Sci. Eng., C* **2007**, *27*, 110.
- [101] H. Wu, L. Zhang, S. Jiang, Y. Zhang, Y. Zhang, C. Xin, S. Ji, W. Zhu, J. Li, Y. Hu, D. Wu, J. Chu, *ACS Appl. Mater. Interfaces* **2020**, *12*, 55390.
- [102] X. Shi, K. Zhang, L. Zhao, B. Jiang, Y. Huang, *Ind. Eng. Chem. Res.* **2021**, *60*, 2154.
- [103] M. D. Bartlett, A. Fassler, N. Kazem, E. J. Markvicka, P. Mandal, C. Majidi, *Adv. Mater.* **2016**, *28*, 3791.
- [104] G. Li, X. Wu, D.-W. Lee, *Sens. Actuators, B* **2015**, *221*, 1114.
- [105] G. Li, D.-W. Lee, *Lab Chip* **2017**, *17*, 3415.
- [106] L. Johnston, J. Yang, J. Han, K. Kalantar-Zadeh, J. Tang, *J. Mater. Chem. C* **2022**, *10*, 921.
- [107] H. Sun, Z. Han, N. Willenbacher, *ACS Appl. Mater. Interfaces* **2019**, *11*, 38092.
- [108] G. Georgousis, C. Pandis, A. Kalamiotis, P. Georgiopoulos, A. Kyritsis, E. Kontou, P. Pissis, M. Micusik, K. Czanikova, J. Kulicek, et al., *Composites, Part B* **2015**, *68*, 162.
- [109] H. Liu, Q. Li, S. Zhang, R. Yin, X. Liu, Y. He, K. Dai, C. Shan, J. Guo, C. Liu, C. Shen, X. Wang, N. Wang, Z. Wang, R. Wei, Z. Guo, *J. Mater. Chem. C* **2018**, *6*, 12121.
- [110] Z. J. Farrell, C. J. Thrasher, A. E. Flynn, C. E. Tabor, *ACS Appl. Nano Mater.* **2020**, *3*, 6297.
- [111] A. Koh, J. Sietins, G. Slipper, R. Mrozek, *J. Mater. Res.* **2018**, *33*, 2443.
- [112] R. E. Calabrese, E. Bury, F. Haque, A. Koh, C. Park, *Composites, Part B* **2022**, *234*, 109686.
- [113] B. J. Blaiszik, S. L. Kramer, M. E. Grady, D. A. McIlroy, J. S. Moore, N. R. Sottos, S. R. White, *Adv. Mater.* **2012**, *24*, 398.
- [114] B. Blaiszik, A. Jones, N. R. Sottos, S. R. White, *J. Microencapsulation* **2014**, *31*, 350.
- [115] J. M. Ginder, M. E. Nichols, L. D. Elie, J. L. Tardiff, in *Smart Structures and Materials 1999: Smart Materials Technologies*, vol. 3675, SPIE, Bellingham, Washington USA **1999**, pp. 131–138.
- [116] A. K. Bastola, M. Hossain, *Composites, Part B* **2020**, *200*, 108348.
- [117] M. Jaafar, F. Mustapha, M. Mustapha, *J. Mater. Res. Technol.* **2021**, *15*, 5010.
- [118] Y. Li, J. Li, W. Li, H. Du, *Smart Mater. Struct.* **2014**, *23*, 123001.
- [119] N. L. Burhannuddin, N. A. Nordin, S. A. Mazlan, S. A. A. Aziz, N. Kuwano, S. K. M. Jamari, Ubaidillah, *Sci. Rep.* **2021**, *11*, 868.

- [120] K. Danas, S. Kankanala, N. Triantafyllidis, *J. Mech. Phys. Solids* **2012**, *60*, 120.
- [121] A. Boczkowska, S. F. Awietjan, *J. Mater. Sci.* **2009**, *44*, 4104.
- [122] O. Padalka, H. Song, N. Wereley, J. Filer II, R. Bell, *IEEE Transactions on Magnetics* **2010**, *46*, 2275.
- [123] S. Tahir, M. Usman, M. A. Umer, *Polymers* **2022**, *14*, 2968.
- [124] R. A. Landa, P. Soledad Antonel, M. M. Ruiz, O. E. Perez, A. Butera, G. Jorge, C. L. Oliveira, R. M. Negri, *J. Appl. Phys.* **2013**, *114*, 21.
- [125] M. Schümann, D. Y. Borin, S. Huang, G. K. Auernhammer, R. Müller, S. Odenbach, *Smart Mater. Struct.* **2017**, *26*, 095018.
- [126] A. S. Semisalova, N. S. Perov, G. V. Stepanov, E. Y. Kramarenko, A. R. Khokhlov, *Soft Matter* **2013**, *9*, 11318.
- [127] W. Hu, G. Z. Lum, M. Mastrangeli, M. Sitti, *Nature* **2018**, *554*, 81.
- [128] A. K. Bastola, M. Paudel, L. Li, W. Li, *Smart Mater. Struct.* **2020**, *29*, 123002.
- [129] J. Zhang, Y. Guo, W. Hu, M. Sitti, *Adv. Mater.* **2021**, *33*, 2100336.
- [130] A. Boczkowska, S. F. Awietjan, S. Pietrzko, K. J. Kurzydłowski, *Composites, Part B* **2012**, *43*, 636.
- [131] M. Sitti, D. S. Wiersma, *Adv. Mater.* **2020**, *32*, 1906766.
- [132] S. Araby, Q. Meng, L. Zhang, H. Kang, P. Majewski, Y. Tang, J. Ma, *Polymer* **2014**, *55*, 201.
- [133] H. Yu, Y. Feng, C. Chen, Z. Zhang, Y. Cai, M. Qin, W. Feng, *Carbon* **2021**, *179*, 348.
- [134] F. Zhang, Y. Feng, W. Feng, *Mater. Sci. Eng.: R: Rep.* **2020**, *142*, 0580.
- [135] A. Heinzl, W. Hering, J. Konys, L. Marocco, K. Litfin, G. Müller, J. Pacio, C. Schroer, R. Stieglitz, L. Stoppel, A. Weisenburger, T. Wetzel, *Energy Technol.* **2017**, *5*, 1026.
- [136] S. H. Jeong, S. Chen, J. Huo, E. K. Gamstedt, J. Liu, S.-L. Zhang, Z.-B. Zhang, K. Hjort, Z. Wu, *Sci. Rep.* **2015**, *5*, 18257.
- [137] M. I. Ralphs, N. Kemme, P. B. Vartak, E. Joseph, S. Tipnis, S. Turnage, K. N. Solanki, R. Y. Wang, K. Rykaczewski, *ACS Appl. Mater. Interfaces* **2018**, *10*, 2083.
- [138] A. Bar-Cohen, K. Matin, S. Narumanchi, *J. Electron. Packag.* **2015**, *137*, 040803.
- [139] Q. Chang, in *Colloid and Interface Chemistry for Water Quality Control*, Academic Press, Cambridge **2016**, pp. 227–245.
- [140] B. Liu, X. Hu, in *Advanced Nanomaterials for Pollutant Sensing and Environmental Catalysis*, Elsevier, Amsterdam **2020**, pp. 1–38.
- [141] S.-Y. Tang, R. Qiao, Y. Lin, Y. Li, Q. Zhao, D. Yuan, G. Yun, J. Guo, M. D. Dickey, T. J. Huang, et al., *Adv. Mater. Technol.* **2019**, *4*, 1800420.
- [142] S.-Y. Tang, B. Ayan, N. Nama, Y. Bian, J. P. Lata, X. Guo, T. J. Huang, *Small* **2016**, *12*, 3861.
- [143] R. W. Style, T. Sai, N. Fanelli, M. Ijavi, K. Smith-Mannschott, Q. Xu, L. A. Wilen, E. R. Dufresne, *Phys. Rev. X* **2018**, *8*, 011028.
- [144] A. A. Sulaimon, B. J. Adeyemi, *Sci. Tech. Behind Nanoemuls.* **2018**, *83*.
- [145] A. Kataruka, S. B. Hutchens, *Soft Matter* **2019**, *15*, 9665.
- [146] L. Marszall, *J. Colloid Interface Sci.* **1977**, *61*, 202.
- [147] S. Handschuh-Wang, M. Rauf, T. Gan, W. Shang, X. Zhou, *ChemistrySelect* **2021**, *6*, 10625.
- [148] J. Ma, Y. Lin, Y.-W. Kim, Y. Ko, J. Kim, K. H. Oh, J.-Y. Sun, C. B. Gorman, M. A. Voinov, A. I. Smirnov, et al., *ACS Macro Lett.* **2019**, *8*, 1522.
- [149] Y. Chen, T. Zhou, Y. Li, L. Zhu, S. Handschuh-Wang, D. Zhu, X. Zhou, Z. Liu, T. Gan, X. Zhou, *Adv. Funct. Mater.* **2018**, *28*, 1706277.
- [150] S. Kanetkar, N. U. H. Shah, R. M. Gandhi, A. Uppal, M. D. Dickey, R. Y. Wang, K. Rykaczewski, *ACS Appl. Eng. Mater.* **2023**.
- [151] H. Wang, B. Yuan, S. Liang, R. Guo, W. Rao, X. Wang, H. Chang, Y. Ding, J. Liu, L. Wang, *Mater. Horiz.* **2018**, *5*, 222.
- [152] S. Liu, M. C. Yuen, E. L. White, J. W. Boley, B. Deng, G. J. Cheng, R. Kramer-Bottiglio, *ACS Appl. Mater. Interfaces* **2018**, *10*, 28232.
- [153] S. Liu, S. N. Reed, M. J. Higgins, M. S. Titus, R. Kramer-Bottiglio, *Nanoscale* **2019**, *11*, 17615.
- [154] S. Liu, S. Y. Kim, K. E. Henry, D. S. Shah, R. Kramer-Bottiglio, *ACS Appl. Mater. Interfaces* **2021**, *13*, 28729.
- [155] M. G. Mohammed, R. Kramer, *Adv. Mater.* **2017**, *29*, 1604965.
- [156] T. R. Lear, S.-H. Hyun, J. W. Boley, E. L. White, D. H. Thompson, R. K. Kramer, *Extreme Mech. Lett.* **2017**, *13*, 126.
- [157] J. W. Boley, E. L. White, R. K. Kramer, *Adv. Mater.* **2015**, *27*, 2355.
- [158] Q. Chen, F. Liang, T. Yang, Q. Li, S. Wu, X.-M. Song, *J. Colloid Interface Sci.* **2022**, *628*, 109.
- [159] S. Y. Ryu, H. Lee, Y. Hong, H. Bandal, M. Goh, H. Kim, J. Lee, *Adv. Mater. Interfaces* **2023**, *10*, 2202527.
- [160] Y. Lin, J. Genzer, W. Li, R. Qiao, M. D. Dickey, S.-Y. Tang, *Nanoscale* **2018**, *10*, 19871.
- [161] S.-Y. Tang, R. Qiao, S. Yan, D. Yuan, Q. Zhao, G. Yun, T. P. Davis, W. Li, *Small* **2018**, *14*, 1800118.
- [162] E. Amstad, M. Chemama, M. Eggersdorfer, L. R. Arriaga, M. P. Brenner, D. A. Weitz, *Lab Chip* **2016**, *16*, 4163.
- [163] P. Lin, Z. Wei, Q. Yan, J. Xie, Y. Fan, M. Wu, Y. Chen, Z. Cheng, *ACS Appl. Mater. Interfaces* **2019**, *11*, 25295.
- [164] F. Zhang, J.-b. Fan, S. Wang, *Angew. Chem., Int. Ed.* **2020**, *59*, 21840.
- [165] E. L. Wittbecker, P. W. Morgan, *J. Polym. Sci.* **1959**, *40*, 289.
- [166] Y. Ming, J. Hu, J. Xing, M. Wu, J. Qu, *J. Microencapsulation* **2016**, *33*, 307.
- [167] X. K. Hillewaere, R. F. Teixeira, L.-T. T. Nguyen, J. A. Ramos, H. Rahier, F. E. Du Prez, *Adv. Funct. Mater.* **2014**, *24*, 5575.
- [168] S. Lu, J. Xing, Z. Zhang, G. Jia, *J. Appl. Polym. Sci.* **2011**, *121*, 3377.
- [169] M. Huang, J. Yang, *J. Mater. Chem.* **2011**, *21*, 11123.
- [170] J. Lee, S. J. Park, C.-S. Park, O. S. Kwon, S. Y. Chung, J. Shim, C.-S. Lee, J. Bae, *Polymers* **2018**, *10*, 675.
- [171] J. Yang, M. W. Keller, J. S. Moore, S. R. White, N. R. Sottos, *Macromolecules* **2008**, *41*, 9650.
- [172] H.-Y. Chao, Microencapsulation by in-situ polymerization of multifunctional epoxy resins, **1986**, US Patent 4, 626, 471.
- [173] X. Liu, X. Sheng, J. K. Lee, M. R. Kessler, *Macromol. Mater. Eng.* **2009**, *294*, 389.
- [174] P. Bolimowski, D. Wass, I. Bond, *Smart Mater. Struct.* **2016**, *25*, 084009.
- [175] B. Blaiszik, N. Sottos, S. White, *Compos. Sci. Technol.* **2008**, *68*, 978.
- [176] Y. C. Yuan, M. Z. Rong, M. Q. Zhang, *Polymer* **2008**, *49*, 2531.
- [177] S. U. Pickering, *J. Chem. Soc., Transactions* **1907**, *91*, 2001.
- [178] Y. Yang, Z. Fang, X. Chen, W. Zhang, Y. Xie, Y. Chen, Z. Liu, W. Yuan, *Front. pharmacology* **2017**, *8*, 287.
- [179] L. Gao, J. He, J. Hu, C. Wang, *ACS Appl. Mater. Interfaces* **2015**, *7*, 25546.
- [180] S. D. Mookhoek, B. J. Blaiszik, H. R. Fischer, N. R. Sottos, S. R. White, S. Van Der Zwaag, *J. Mater. Chem.* **2008**, *18*, 5390.
- [181] S. Y. Kim, Y. Choo, R. A. Bilodeau, M. C. Yuen, G. Kaufman, D. S. Shah, C. O. Osuji, R. Kramer-Bottiglio, *Sci. Rob.* **2020**, *5*, eaay3604.
- [182] C. Li, J. Tan, H. Li, D. Yin, J. Gu, B. Zhang, Q. Zhang, *Polym. Chem.* **2015**, *6*, 7100.
- [183] B. P. Binks, D. Yin, *Soft Matter* **2016**, *12*, 6858.
- [184] I. Gurevitch, M. S. Silverstein, *Macromolecules* **2012**, *45*, 6450.
- [185] D. Sun, Y. B. Chong, K. Chen, J. Yang, *Chem. Eng. J.* **2018**, *346*, 289.
- [186] S. Norliana, A. Abdulamir, F. Abu Bakar, A. Salleh, *American J. Pharmacol. Toxicol.* **2009**, *4*, 98.
- [187] G. León, N. Paret, P. Fankhauser, D. Grenno, P. Erni, L. Ouali, D. Berthier, *RSC Adv.* **2017**, *7*, 18962.
- [188] Y. Xu, Y. Su, X. Xu, B. Arends, G. Zhao, D. N. Ackerman, H. Huang, S. P. Reid, J. L. Santaripa, C. Kim, Z. Chen, S. Mahmoud, Y. Ling, A. Brown, Q. Chen, G. Huang, J. Xie, Z. Yan, *Sci. Adv.* **2023**, *9*, eadf0575.
- [189] X. He, T. Xuan, J. Wu, H. Pang, H. Deng, S. Xuan, X. Gong, *ACS Appl. Mater. Interfaces* **2023**, *15*, 5856.
- [190] X. Xue, D. Zhang, Y. Wu, R. Xing, H. Li, T. Yu, B. Bai, Y. Tao, M. D. Dickey, J. Yang, *Adv. Funct. Mater.* **2023**, *33*, 2210553.

- [191] E. J. Krings, H. Zhang, S. Sarin, J. E. Shield, S. Ryu, E. J. Markvicka, *Small* **2021**, *17*, 2104762.
- [192] J. D. Eshelby, *Proc. royal soc. London. Series A. Math. phys. sci.* **1957**, *241*, 376.
- [193] Z. Hashin, S. Shtrikman, *J. Mech. Phys. Solids* **1963**, *11*, 127.
- [194] T. Mori, K. Tanaka, *Acta Metall.* **1973**, *21*, 571.
- [195] M. Loos, *Carbon nanotube reinforced composites* **2015**, pp. 125–170.
- [196] R. W. Style, R. Boltyanskiy, B. Allen, K. E. Jensen, H. P. Foote, J. S. Wettlaufer, E. R. Dufresne, *Nat. Phys.* **2015**, *11*, 82.
- [197] R. W. Style, J. S. Wettlaufer, E. R. Dufresne, *Soft Matter* **2015**, *11*, 672.
- [198] M. D. Bartlett, A. Fassler, N. Kazem, E. J. Markvicka, P. Mandal, C. Majidi, *Adv. Mater.* **2016**, *28*, 3726.
- [199] P. S. Owuor, S. Hiremath, A. C. Chipara, R. Vajtai, J. Lou, D. R. Mahapatra, C. S. Tiwary, P. M. Ajayan, *Adv. Mater. Interfaces* **2017**, *4*, 1700240.
- [200] M. J. Ford, M. Palaniswamy, C. P. Ambulo, T. H. Ware, C. Majidi, *Soft Matter* **2020**, *16*, 5878.
- [201] A. Mohammadi Nasab, T. L. Buckner, B. Yang, R. Kramer-Bottiglio, *Adv. Mater. Technol.* **2022**, *7*, 2100920.
- [202] T. L. Buckner, Z. J. Farrell, A. M. Nasab, R. Kramer-Bottiglio, *J. Compos. Mater.* **2023**, *57*, 619.
- [203] N. Kazem, M. D. Bartlett, C. Majidi, *Adv. Mater.* **2018**, *30*, 1706594.
- [204] C. Chiew, M. H. Malakooti, *Compos. Sci. Technol.* **2021**, *208*, 108752.
- [205] A. Mohammadi Nasab, S. Sharifi, S. Chen, Y. Jiao, W. Shan, *Adv. Intell. Syst.* **2021**, *3*, 2000166.
- [206] S. C. Cheng, R. Vachon, *Int. J. Heat Mass Transfer* **1969**, *12*, 249.
- [207] D. Bruggeman, *Ann. Phys.* **1935**, *416*, 636.
- [208] N. Phan-Thien, D. Pham, *J. Non-Newtonian Fluid Mech.* **1997**, *72*, 305.
- [209] Y. Agari, T. Uno, *J. Appl. Polym. Sci.* **1986**, *32*, 5705.
- [210] H. J. Mea, L. Delgadillo, J. Wan, *Proc. Natl. Acad. Sci. USA* **2020**, *117*, 14790.
- [211] E. J. Barron III, R. S. Peterson, N. Lazarus, M. D. Bartlett, *ACS Appl. Mater. Interfaces* **2020**, *12*, 50909.
- [212] L. Teng, L. Zhu, S. Handschuh-Wang, X. Zhou, *J. Mater. Chem. C* **2019**, *7*, 15243.



Sophia Eristoff is a graduate student in the department of Mechanical Engineering and Materials Science at Yale University and a NASA space technology graduate research fellow. She earned her B.S. in materials science and engineering and biomedical engineering at Carnegie Mellon University. Her interests primarily lie in creating soft materials that possess unique stimuli-responsive properties to enable advantageous functionalities. Additional interests include polymer synthesis, composites manufacturing, and potential applications in biotechnology.



Amir Mohammadi Nasab received his B.S. in aerospace engineering from Amirkabir University of Technology and his M.S. in mechanical engineering from Iran University of Science and Technology. He completed his Ph.D. degree in mechanical engineering at the University of Nevada-Reno under the supervision of Professor Wanliang Shan. Subsequently, he held a postdoctoral position in mechanical engineering and material science at Yale University in Professor Rebecca Kramer-Bottiglio's lab. His research contributed to the fields of soft robotics, adhesion mechanics, thermodynamics, and multifunctional composites.



Xiaonan Huang is an Assistant Professor in the Robotics Department at the University of Michigan, Ann Arbor, specializing in autonomous dynamic soft robots for challenging environments. He earned his Ph.D. and M.S. in Mechanical Engineering from Carnegie Mellon University in 2020 and 2016, and a B.S. in Mechanical Engineering and B.A. in Japanese from Harbin Institute of Technology in 2014 and 2013. His notable publications include works in *Science Robotics*, *Nature Communication*, *Nature Materials*, *Nature Electronics*, *PNAS*, *Advanced Materials Technologies*, *Soft Robotics*, and *Robotics and Automation Letters*.



Rebecca Kramer-Bottiglio is the John J. Lee Associate Professor of Mechanical Engineering and Materials Science at Yale University. Focusing on the intersection of materials, manufacturing, and robotics, her group is deriving new multifunctional materials that will allow next-generation robots to adapt their properties, morphology, and control policy to changing tasks and environments. She is a recipient of the NSF Career award, NASA Early Career award, AFOSR Young Investigator award, ONR Young Investigator award, and Presidential Early Career Award for Scientists and Engineers (PECASE). She was named a National Academy of Engineering (NAE) Gilbreth Lecturer in 2022 and a National Academy of Science (NAS) Kavli Fellow in 2023.